Multiple phage resistance systems inhibit infection via SIR2-dependent NAD+ depletion

Multiple phage resistance systems inhibit infection via SIR2-dependent NAD^+ depletion

Jeremy Garb[1], Anna Lopatina[1,‡], Aude Bernheim[1,#], Mindaugas Zaremba[2], Virginijus Siksnys[2], Sarah Melamed[1], Azita Leavitt[1], Adi Millman[1], Gil Amitai[1], Rotem Sorek[1,*]

[1]Department of Molecular Genetics, Weizmann Institute of Science, Rehovot 7610001, Israel

[2] Institute of Biotechnology, Life Sciences Center, Vilnius University, Sauletekio al. 7, LT-10257 Vilnius, Lithuania

[‡] Present address: Division of Microbial Ecology, Department of Microbiology and Ecosystem Science, Center for Microbiology and Environmental Systems Science, University of Vienna, Vienna, Austria.

[#] Present address: SEED, U1284, INSERM, Université Paris Cité, Paris, France.

[*]correspondence: rotem.sorek@weizmann.ac.il

Abstract

Defense-associated sirtuins (DSR) comprise a family of proteins that defend bacteria from phage infection via an unknown mechanism. These proteins are common in bacteria and harbor an N-terminal sirtuin (SIR2) domain. In this study we report that DSR proteins degrade nicotinamide adenine dinucleotide (NAD^+) during infection, depleting the cell of this essential molecule and aborting phage propagation. Our data show that one of these proteins, DSR2, directly identifies phage tail tube proteins and then becomes an active NADase in *Bacillus subtilis*. Using a phage mating methodology that promotes genetic exchange between pairs of DSR2-sensitive and DSR2–resistant phages, we further show that some phages express anti-DSR2 proteins that bind and repress DSR2. Finally, we demonstrate that the SIR2 domain serves as an effector NADase in a diverse set of phage defense systems outside the DSR family. Our results establish the general role of SIR2 domains in bacterial immunity against phages.

Introduction

SIR2-domain proteins, or sirtuins, are found in organisms ranging from bacteria to humans. These proteins have been widely studied in yeast and mammals, where they were shown to regulate transcription repression, recombination, DNA repair and cell cycle processes [1]. In eukaryotes, SIR2 domains were shown to possess enzymatic activities, and function either as protein deacetylases or ADP ribosyltransferases [2,3]. In both cases, the SIR2 domain utilizes nicotinamide adenine dinucleotide (NAD^+) as a cofactor for the enzymatic reaction [4].

In bacteria, SIR2 domains were recently shown to participate in defense systems that protect against phages. These domains are associated with multiple different defense systems, including prokaryotic argonautes (pAgo) [5], Thoeris [6,7], AVAST, DSR, and additional systems [8]. It was recently shown that the SIR2 domain in the Thoeris defense system is an NADase responsible for depleting NAD^+ from the cell once phage infection has been sensed [7]. However, it is currently unknown whether SIR2 domains in other defense systems perform a similar function, or whether they have other roles in phage defense.

Results

DSR2 defends against phage SPR via abortive infection

To study the role of SIR2 domains in bacterial anti-phage defense, we began by focusing on DSR2, a minimal defense system that includes a single protein with an N-terminal SIR2 domain and no additional identifiable domains (Fig. 1A). The DSR2 gene family was recently identified based on a screen for genes commonly found in bacterial anti-phage defense islands [8]. We cloned the DSR2 gene from *Bacillus subtilis* 29R, under the control of its native promoter, into the genome of *B. subtilis* BEST7003 which naturally lacks this gene, and challenged the DSR2-containing strain with a set of phages from the SPbeta family. We found that DSR2 protected *B. subtilis* against phage SPR, reducing plating efficiency by four orders of magnitude (Fig. 1B, Extended Data Fig.1). Point mutations in residues N133 and H171 in DSR2, both of which predicted to disable the active site of the SIR2 domain, abolished defense, suggesting that the enzymatic activity of SIR2 is essential for DSR2 defense (Fig. 1B).

We next tested whether DSR2 defends via abortive infection, a process that involves premature death or growth arrest of the infected cell, preventing phage replication and spread to nearby cells [9]. When infected in liquid media, DSR2-containing bacterial cultures collapsed if the culture was infected by phage in high multiplicity of infection (MOI), similar to DSR2-lacking cells (Fig. 1C). However, despite collapsing the culture, phages were not able to replicate on DSR2-containing cells (Extended Data Fig.2). In low MOI infection, DSR2-lacking control cultures collapsed but DSR2-containing bacteria survived (Fig. 1C). This phenotype is a hallmark of abortive infection, in which infected bacteria that contain the defense system do not survive but also do not produce phage progeny [9].

DSR2 depletes NAD^+ upon phage infection

To ask whether DSR2 manipulates the NAD^+ content of the cell during phage infection, we used mass spectrometry to monitor NAD^+ levels in infected cells at various time points following initial

infection. When DSR2-containing cells were infected by phage SPR, cellular NAD^+ decreased sharply between 20 and 30 minutes from the onset of infection (Fig. 1D). NAD^+ levels did not change in cells in which the SIR2 active site was mutated, or in DSR2-lacking control cells, suggesting that the SIR2 domain is responsible for the observed NAD^+ depletion (Fig. 1D). In parallel with NAD^+ depletion, we observed accumulation of the product of NAD^+ cleavage, ADP-ribose (ADPR) (Fig. 1E). These results demonstrate that DSR2 is an abortive infection protein that causes NAD^+ depletion in infected cells.

DSR2 strongly protected *B. subtilis* cells against SPR, a phage belonging to the SPbeta group of phages [10] (Fig. 1B, Extended Data Fig.1). However, the defense gene failed to protect against phages phi3T and SPbeta, although both these phages belong to the same phage group as SPR (Fig. 1B). This observation suggests that phages phi3T and SPbeta either encode genes that inhibit DSR2, or lack genes that are recognized by DSR2 and trigger its NADase activity. The phages SPR, phi3T and SPbeta all share substantial genomic regions with high sequence homology (Fig. 2A). We therefore reasoned that co-infecting cells with two phages, either SPR and phi3T, or SPR and SPbeta, may result in recombination-mediated genetic exchange between the phages, which would enable pinpointing genes that allow escape from DSR2 defense when acquired by SPR (Fig. 2B). Such crossing techniques were previously successful in pinpointing genetic phenotypes in phages [11,12].

To generate a bacterial host that would select for such genetic exchange events, we cloned into DSR2-containing cells an additional defense protein, a prokaryotic viperin homolog (pVip) from *Fibrobacter* sp. UWT3 [13]. The pVip protein, when expressed alone in *B. subtilis*, protected it from phi3T and SPbeta but not from SPR, a defense profile which is opposite to that of the DSR2 profile in terms of the affected phages (Extended Data Fig.3). Accordingly, none of the three SPbeta-group phages could form plaques on the strain that expressed both defensive genes. However, when simultaneously infecting the double defense strain with SPR and either phi3T or SPbeta, plaque forming hybrids were readily obtained, indicating that these hybrid phages recombined and acquired a combination of genes enabling them to escape both DSR2 and pVip (Fig. 2C).

A phage-encoded anti-DSR2 protein

We isolated and sequenced 32 such hybrid phages, assembled their genomes, and compared these genomes to the genome of the parent SPR phage (Fig. 2D; Supplementary File 1). This led to the identification of two genomic segments that were repeatedly acquired by SPR phages. Acquisition of either of these segments from a genome of a co-infecting phage rendered SPR resistant to DSR2 (Fig. 2D). The first segment included five small genes of unknown function that are present in phages phi3T and SPbeta but not in the wild type SPR phage, and we therefore tested whether any of these genes was capable of inhibiting DSR2. One of the genes, when co-expressed with DSR2, rendered DSR2 inactive, suggesting that this phage gene encodes an anti-DSR2 protein (Fig. 3A). The other four genes in the segment did not inhibit DSR2 defense (Extended Data Fig.4A). The DSR2-inhibiting protein, which we named DSAD1 (DSR Anti Defense 1), is 120aa long and has no identifiable sequence homology to proteins of known function. Co-expression of DSR2 and tagged DSAD1, followed by pulldown assays, showed direct interaction between the two proteins (Fig. 3B). These results indicate that DSAD1 is a phage protein that binds and inhibits DSR2.

DSR2 is activated by phage tail tube protein

We next examined the second genomic segment that, when acquired, allowed phage hybrids to escape DSR2. In the parent SPR phage, this region spans three operons encoding a set of phage structural proteins, including capsid and tail proteins. Hybrid phages in which the original genes were replaced by their homologs from SPbeta or phi3T become resistant to DSR2 (Fig. 2D). We hypothesized that one of the structural proteins in phage SPR is recognized by DSR2 to activate its defense, and when this protein is replaced by its homolog from another phage, recognition no longer occurs. To test this hypothesis, we attempted to clone each of the three operons found in the original DNA segment in SPR into *B. subtilis* cells that also express DSR2. One of these operons could not be cloned into DSR2-expressing cells, and we then repeated the cloning attempt for each of the genes in the operon. One of these genes, encoding a tail tube protein, could not be cloned into DSR2-expressing cells but was readily cloned into cells in which the DSR2 active site was mutated (Fig. 3C, Extended Data Fig.4B-C).

To further test if co-expression of DSR2 and the SPR tail tube protein is toxic to bacteria, we cloned each of these genes under an inducible promoter within *E. coli* cells. In support of our hypothesis, growth was rapidly arrested in cells in which the expression of both genes was induced (Fig. 3D), and these cells became depleted of NAD^+ (Fig. 3E, 3F). Furthermore, pulldown assays with tagged proteins showed that DSR2 directly binds the tail tube protein of phage SPR (Fig. 3B). The tail tube protein was not able to pull down DSR2 when DSAD1 was coexpressed in the same cells, suggesting that the tail tube protein and DSAD1 are competitive binders for DSR2 (Extended Data Fig.5). These results demonstrate that the tail tube protein of phage SPR is directly recognized by the defense protein DSR2, and that this recognition triggers the NADase activity of DSR2 and results in growth arrest (Fig. 3G).

The original tail tube protein of phage SPR is substantially divergent from its counterparts from phages SPbeta or phi3T, sharing only ~40% amino acid sequence identity with these proteins (Extended Data Fig.6). This divergence explains why the replacement of the original SPR protein with its SPbeta homolog renders the hybrid phage resistant to DSR2. In support of this, the tail tube protein of phage SPbeta showed much weaker ability to pull down DSR2 as compared to the tail tube counterpart from phage SPR (Fig. 3B). Presumably, the evolutionary pressure imposed by DSR2 and other bacterial defense systems that recognize tail tube proteins has led to the observed diversification in these proteins in phages of the SPbeta group.

Various defense systems with SIR2 domains deplete NAD^+ upon infection

Our results show that DSR2 exerts its defensive activity by depleting NAD^+ from infected cells. NADase activity was also recently described in the Thoeris defense system, in which a small molecule signal activates a SIR2-encoding effector to deplete NAD^+ once phage infection has been recognized [7]. To test if NAD^+ depletion is a general activity of SIR2 domains in bacterial defense systems, we examined three additional defense systems that contain a SIR2 domain (Fig. 4A). These systems included a two-gene system that encodes, in addition to the SIR2 domain, also a prokaryotic argonaute homolog (pAgo), a two-gene system that encodes a HerA-like DNA translocase [8], and a single SIR2-domain protein called DSR1 [8] (Fig. 4A). DSR1 was cloned into *B. subtilis* BEST7003, while the other two systems were cloned into an *E. coli* host. Consistent with our hypothesis, these systems defended against multiple different phages (Fig. 4B, Extended Data Fig.7), and NAD^+ depletion was observed in each case (Fig. 4C-E). Mutations inactivating

the HerA-like DNA translocase or the pAgo protein abolished defense, indicating that these two proteins also participate in the defensive function (Extended Data Fig.8). Liquid infection with high and low MOIs showed a phenotype consistent with abortive infection for the SIR2/pAgo and the SIR2-HerA systems (Fig. 4F-G). However, the DSR1 protein seems to inhibit the replication of phage phi29 without arresting the growth of the bacterial cells, and depletion of NAD^+ was only transient (Fig. 4E, 4H). Together, these results demonstrate a general role of SIR2 domains as NAD^+ depleting effectors in bacterial defense against phage.

Discussion

Our data suggest that NAD^+ depletion is a canonical function for SIR2 domains within bacterial defense systems. We show that four anti-phage defense systems, all containing SIR2 domains but otherwise comprising different architectures, deplete NAD^+ in response to phage infection. Specifically, in the case of DSR2, we show that this protein recognizes newly translated phage tail tube proteins to become an active NADase. Phages of the SPbeta family have at least two versions of the tail tube protein, and only certain alleles are strongly recognized by DSR2. In addition, we found that some phages in this family carry a small protein, DSAD1, which binds and inactivates DSR2.

NAD^+ depletion was previously shown to be toxic to bacterial cells [14–17], and it was recently demonstrated in the Thoeris, CBASS and Pycsar systems that defense involving NAD^+ depletion during phage infection is associated with an eventual cell death [7,15,18]. Indeed, in three out of the four SIR2-containing systems that we studied, growth arrest or death of the bacterial host was observed in response to phage infection. However, DSR1 protection from phage phi29 did not involve culture collapse (Fig. 4H). Furthermore, our data show that the NAD^+ levels in cells containing DSR1 recovered after the initial depletion (Fig. 4E). It is possible that in some cases, reversible reduction of NAD^+ to low but not zero levels may be enough to interfere with phage replication while still allowing cell growth. Alternatively, lowered levels of NAD^+ might have different outcomes for the infected cell depending on additional components derived from the infecting phage.

The molecular signatures recognized by abortive infection defense systems as an indication for phage infection have been notoriously challenging to discover. In a minority of cases where the trigger was discovered, it was shown that some systems "guard" an immunity hub in the cell, and become triggered when the phage tampers with the immunity complex [19,20]. In other cases, a specific protein expressed by the phage during infection forms the trigger for system activation, as shown for the *Staphylococcus* Stk2 abortive infection kinase [21], and also as we show for DSR2 in the current study. However, the SPR tail tube protein that activates DSR2 does not activate DSR1, suggesting that these two proteins recognize different molecular signatures (Extended Data Fig.9). The mechanisms by which phages activate, and potentially inhibit, the other three SIR2-domain-containing systems described in this study remains to be elucidated by future studies.

The arsenal of defense mechanisms known to protect bacteria against phage has recently been substantially expanded following the discovery of dozens of new anti-phage defense systems [6,8,22]. While the mechanism of defense was deciphered for some of these systems [7,13,18,23], in many cases it is not known what molecular patterns of the phage trigger these systems to become active. In the

current study we used a "phage mating" technique, which was previously successfully used in other studies [11,12], to promote genetic exchange between phages that are sensitive to the defense system and phages that can overcome it. Genome analyses of hybrid phages enabled us to pinpoint the exact phage proteins that activate or repress DSR2. We believe that the phage mating approach should be a useful tool for other studies attempting to identify phage triggers of bacterial defense systems.

Methods

Bacterial strains and phages

B. subtilis strain BEST7003 (obtained from I. Mitsuhiro at Keio University, Japan) was grown in MMB (LB + 0.1 mM MnCl2 + 5 mM $MgCl_2$, with or without 0.5% agar) at 30 °C. Whenever applicable, media were supplemented with spectinomycin (100 µg/ml) and chloramphenicol (5 µg/ml), to ensure selection of transformed and integrated cells. *E. coli* strain MG1655 (ATCC 47076) was grown in MMB at 37 °C. Whenever applicable, media were supplemented with ampicillin (100 µg/ml) or chloramphenicol (30 µg/ml) or kanamycin (50 µg/ml), to ensure the maintenance of plasmids. Phages used in this study are listed in Table 1.

Plasmid and strain construction

Details on defense systems analyzed in this study are summarized in Table 2, and sequences of primers used in this study are in Supplementary Table S3. Defense systems DSR1, DSR2, and SIR2-HerA were synthesized by Genscript Corp. and cloned into the pSG1 plasmid [6] together with their native promoters. A whole operon of the SIR2/pAgo system, composed of the genes encoding the SIR2 (GSU1360, NP_952413.1) and pAgo (GSU1361, NP_952414.1) proteins, was amplified by PCR using the oligonucleotides MZ239 and MZ240, respectively, from the genomic DNA of *Geobacter sulfurreducens* Caccavo (LGC Standards cat #51573D-5). The resulting DNA fragment was digested by Eco31I (ThermoFisher cat #FD0293) and XhoI (ThermoFisher cat #FD0694) and using T4 DNA ligase (ThermoFisher cat #EL0014) was cloned into pBAD/HisA expression vector (ThermoFisher cat #V43001) precleaved with NheI (ThermoFisher cat #FD0973) and XhoI and dephosphorylated using FastAP (ThermoFisher cat #EF0651). The GsSir2 protein contains a His_6-Tag at its N terminus. The mutants DSR2 (N133A) and DSR2 (H171A) were constructed using the Q5 Site-directed Mutagenesis kit (NEB, E0554S) using either primers JG216 and JG217, or JG220 and JG221 respectively. The mutant DSR1 (H194A) was constructed using the Q5 Site-directed Mutagenesis kit using primers JG496 and JG497. The mutant SIR2-HerA (SIR2 D165A H212A) was constructed by first using the Q5 Site-directed Mutagenesis kit using primers JG498 and JG499 to introduce the D165A mutation, and then using the resulting plasmid for further Q5 Site-directed Mutagenesis and the introduction of the second H212A mutation using primers JG500 and JG501. The mutant SIR2-HerA (HerA K167A) was constructed using the Q5 Site-directed Mutagenesis kit using primers JG502 and JG503. The mutant SIR2/pAgo (SIR2 N142A) was constructed using the Q5 Site-directed Mutagenesis kit using primers JG463 and JG464.To inactivate the GsAgo protein a bulky His_6-**S**trepII-His_6-tag (HSH-tag, 29 aa.: LEGHHHHHHSSWSHPQFEKGVEGHHHHHH) was fused to its C terminus. For this, a whole operon of the GsSir2/Ago system was amplified by PCR using the oligonucleotides MZ-325 and MZ-326, respectively, from the genomic DNA. The resulting DNA fragment was digested by Eco31I and XhoI and using T4 DNA ligase was cloned into pBAD24-HSH expression vector

precleaved with NcoI (ThermoFisher cat#FD0573) and XhoI and dephosphorylated using FastAP. In this case, the GsSir2 protein does not contain any tag at its N-terminus.

A cloning shuttle vector for large fragments was constructed by Genscript Corp. This vector was constructed by replacing the Pxyl promoter and its downstream open reading frame in plasmid pGO1_thrC_Pxyl_cereus_ThsA [7], with a synthesized Phspank sfGFP cassette taken from pDR111 [24], resulting in the plasmid pSG-thrC_Phspank_sfGFP (Supplementary File S2). The vector contains a p15a origin of replication and ampicillin resistance for plasmid propagation in *E. coli*, and a thrC integration cassette with chloramphenicol resistance for genomic integration into *B. subtilis*.

DSAD1 from SPbeta (NCBI protein accession WP_004399562) and phage tail tube protein from SPR (NCBI protein accession WP_010328117) were amplified from phage genomic DNA using primers JG346 and JG347 (for DSAD1) and JG142 and JG143 (for tail tube), and cloned into the pSG-thrC_Phspank_sfGFP vector, replacing sfGFP. The vector backbone was amplified using primers JG13 and JG14.

The additional DSR2 activator candidates tested in this research were also amplified from phage SPR genomic DNA and cloned into the pSG-thrC_Phspank_sfGFP vector, replacing sfGFP. “Operon 1” was lifted with JG431 and J432. “Operon 2” was lifted with JG433 and JG434. “Operon 3” was lifted with JG435 and JG436. “gene 5” was lifted with JG437 and JG438. “gene 6” was lifted with JG439 and JG440. “gene 7” was lifted with JG441 and JG442.

In a similar fashion, the additional DSR2 inhibition candidates tested in this paper were amplified from phage SPbeta. “gene 1” was lifted with JG134 and JG183. “gene 2” was lifted with JG184 and JG185. “gene 3” was lifted with JG186 and JG187. “gene 4” was lifted with JG188 and JG189.

For expression in *E. coli MG1655*, DSR2 and DSR2(H171A) were amplified and cloned into the plasmid pBbA6c-RFP (Addgene, cat. #35290) using primers JG259 and JG260. The SPR tail tube gene was amplified from phage genomic DNA and cloned into the plasmid pBbS8k-RFP (Addgene, cat. #35276) with primers JG249 and JG250 for inducible expression in *E. coli*.

For the assembly of tagged protein constructs, a pBbS8k with sfGFP fused to a C-terminal TwinStrep tag was first constructed (Supplementary File S3). The pBbS8k vector backbone was amplified using primers JG406 and JG407, and the sfGFP with a C-terminal TwinStrep tag was amplified from an *amyE* shuttle vector pGO6_amyE_hspank_GFP [7] with primers JG366 and JG367 and cloned into the pBbS8k plasmid, replacing RFP. To create the C-terminally-tagged SPR tail tube, SPbeta tail tube and DSAD1 constructs, the genes were amplified from phage genomic DNA using primers JG408 and JG409 (for SPR tail tube), JG421 and JG422 (for SPbeta tail tube) and JG410 and JG411 (for DSAD1) and cloned into the pBbS8k sfGFP with C-terminal TwinStrep mentioned above, replacing sfGFP. For this, the pBbS8k with C-terminal TwinStrep vector backbone was amplified using primers JG407 and JG412.

For the assembly of a DSAD1 gene containing plasmid which is compatible with both pBbS8k and pBbA6c, DSAD1 gene was lifted from phage SPbeta genomic DNA using primers JG429 and

JG430 and Gibson assembled with a backbone amplified from plasmid pAraGFPCDF (Addgene, cat. #47516) with primers JG427 and JG428.

To assemble a constitutively expressed pVip construct to be integrated into the thrC site of *B. subtilis*, first the pVip gene was lifted from the plasmid reported in [13] using primers JG3 and JG4 and Gibson assembled with a backbone amplified from plasmid pJMP4 (provided by J. M. Peters) with primers JG1 and JG2. From the resulting plasmid, pVIP was lifted with the Pveg promoter using primers JG82 and JG83 and Gibson assembled with a backbone amplified from pSG-thrC_Phspank_sfGFP using primers JG81 and OGO603.

All PCR reactions were performed using KAPA HiFi HotStart ReadyMix (Roche cat # KK2601). Cloning was performed using the NEBuilder HiFi DNA Assembly kit (NEB, E2621).

Bacillus transformation

Transformation to *B. subtilis* BEST7003 was performed using MC medium as previously described [25]. MC medium was composed of 80 mM K_2HPO_4, 30 mM KH_2PO_4, 2% glucose, 30 mM trisodium citrate, 22 µg/ml ferric ammonium citrate, 0.1% casein hydrolysate (CAA), 0.2% sodium glutamate. From an overnight starter of bacteria, 10 µl were diluted in 1 ml of MC medium supplemented with 10 µl 1M $MgSO_4$. After 3 hours of incubation (37°C, 200 rpm), 300 µl of the culture was transferred to a new 15 ml tube and ~200 ng of plasmid DNA was added. The tube was incubated for another 3 hours (37°C, 200 rpm), and the entire reaction was plated on Lysogeny Broth (LB) agar plates supplemented with 5 µg/ml chloramphenicol or 100 µg/ml spectinomycin and incubated overnight at 30°C.

Plaque assays

Phages were propagated by picking a single phage plaque into a liquid culture of *B. subtilis* BEST7003 or *E. coli* MG1655 grown at 37°C to OD_{600} 0.3 in MMB medium until culture collapse. The culture was then centrifuged for 10 minutes at 3,200 x *g* and the supernatant was filtered through a 0.2 µm filter to get rid of remaining bacteria and bacterial debris. Lysate titer was determined using the small drop plaque assay method as previously described [26].

Plaque assays were performed as previously described [6,26]. Bacteria containing defense system and control bacteria with no system were grown overnight at 37°C. Then 300 µl of the bacterial culture was mixed with 30 ml melted MMB 0.5% agar, poured on 10 cm square plates, and let to dry for 1 hour at room temperature. For cells that contained inducible constructs, the inducers were added to the agar before plates were poured. 10-fold serial dilutions in MMB were performed for each of the tested phages and 10 µl drops were put on the bacterial layer. After the drops had dried up, the plates were inverted and incubated overnight at room temperature or 37°C. Plaque forming units (PFUs) were determined by counting the derived plaques after overnight incubation and lysate titer was determined by calculating PFUs per ml. When no individual plaques could be identified, a faint lysis zone across the drop area was considered to be 10 plaques. Details of specific conditions used in plaque assays for each defense system are found in Table 2.

Liquid culture growth assays

Non-induced overnight cultures of bacteria containing defense system and bacteria with no system (negative control) were diluted 1:100 in MMB medium supplemented with appropriate antibiotics

and incubated at 37°C while shaking at 200 rpm until early log phase (OD_{600} = 0.3). 180 µl of the culture were then transferred into wells in a 96-well plate containing 20 µl of phage lysate for a final MOI of 10 and 0.1 for phage lambda(vir), an MOI of 4 and 0.04 for phages SPR, phi29 and vB_EcoM-KAW1E185, or 20 µl of MMB for uninfected control. Infections were performed in triplicates from overnight cultures prepared from separate colonies. Plates were incubated at 30°C or 37°C (as indicated) with shaking in a TECAN Infinite200 plate reader and an OD_{600} measurement was taken every 10 min. Details of specific conditions used for each defense system are found in Table 2.

Liquid culture growth toxicity assays

Non-induced *E. coli* MG1655 with DSR2 and tail tube, or DSR2 and RFP (negative control), were grown overnight in MMB supplemented with 1% glucose and the appropriate antibiotics. Cells were diluted 1:100 in 3 ml of fresh MMB and grown at 37°C to an OD_{600} of 0.3 before expression was induced. The inducers were then added to a final concentration of 0.2% arabinose and 1mM IPTG, and MMB was added instead for the uninduced control cells. The cells were transferred into a 96-well plate. Plates were incubated at 37°C with shaking in a TECAN Infinite200 plate reader with an OD_{600} measurement was taken every 10 min.

Infection time course phage titer assay

Non-induced overnight cultures of bacteria containing the DSR2 gene and bacteria with no system (negative control) were diluted 1:100 in 3 ml MMB medium and incubated at 37°C while shaking at 200 rpm until early log phase (OD_{600} = 0.3), and then cultures were infected with phage SPR at an MOI of 4. Cultures were left shaking at 37°C for the duration of the experiment. At each time point, 1 ml of culture was filtered through a 0.2 µm filter (Whatman cat# 10462200) and then used in an infection plaque assay on *B. subtilis* BEST7003 at room temperature. The sample for time 0 was produced my mixing the same amount of phage used for infection in 3 ml MMB medium.

Cell lysate preparation for LC-MS

Overnight cultures of bacteria containing defense systems and bacteria with no system (negative control) were diluted 1:100 in 250 ml MMB and incubated at 37°C with shaking (200 rpm) until reaching OD_{600} of 0.3. For cells that contained inducible SIR2/pAgo constructs, the inducers were added at an OD_{600} of 0.1. A sample of 50 ml of uninfected culture (time 0) was then removed, and phage stock was added to the culture to reach an MOI of 5-10. Flasks were incubated at 30°C or 37°C (as indicated) with shaking (200 rpm) for the duration of the experiment. 50 ml samples were collected at various time points post infection. Immediately upon sample removal the sample tube was placed in ice, and centrifuged at 4°C for 5 minutes to pellet the cells. The supernatant was discarded and the tube was frozen at -80°C. To extract the metabolites, 600 µl of 100 mM phosphate buffer at pH 8, supplemented with 4 mg/ml lysozyme, was added to each pellet. Tubes were then incubated for 30 minutes at RT, and returned to ice. The thawed sample was transferred to a FastPrep Lysing Matrix B 2 ml tube (MP Biomedicals cat # 116911100) and lysed using FastPrep bead beater for 40 seconds at 6 m/s. Tubes were then centrifuged at 4°C for 15 minutes at 15,000 *g*. Supernatant was transferred to Amicon Ultra-0.5 Centrifugal Filter Unit 3 KDa (Merck Millipore cat # UFC500396) and centrifuged for 45 minutes at 4°C at 12,000 *g*. Filtrate was taken and used for LC-MS analysis. Details of specific conditions used for each defense system are found in Table 2.

Quantification of NAD^+ and ADPR by HPLC-MS

Cell lysates were prepared as described above and analyzed by LC-MS/MS. Quantification of metabolites was carried out using an Acquity I-class UPLC system coupled to Xevo TQ-S triple quadrupole mass spectrometer (both Waters, US). The UPLC was performed using an Atlantis Premier BEH C18 AX column with the dimension of 2.1 × 100 mm and particle size of 1.7 µm (Waters). Mobile phase A was 20 mM ammonium formate at pH 3 and acetonitrile was mobile phase B. The flow rate was kept at 300 µl min^{-1} consisting of a 2 min hold at 2% B, followed by linear gradient increase to 100% B during 5 min. The column temperature was set at 25°C and an injection volume of 1 µl. An electrospray ionization interface was used as ionization source. Analysis was performed in positive ionization mode. Metabolites were detected using multiple-reaction monitoring, using argon as the collision gas. Quantification was made using standard curve in 0–1 mM concentration range. NAD+ (Sigma, N0632-1G) and ADPR (Sigma, A0752-25MG) were added to standards and samples as internal standard (0.5 µM). TargetLynx (Waters) was used for data analysis.

Pulldown assays

Non-induced overnight cultures of *E. coli* MG1655 with DSR2 (H171A), DSAD1, DSAD1 with C-terminal TwinStrep tag, SPR tail tube protein with C-terminal TwinStrep tag, or combinations of these proteins were diluted 1:100 in 50 ml of MMB and grown at 37°C to an OD_{600} of 0.3. Expression was then induced by adding 0.2% arabinose and 1mM IPTG, and cells continued to grow to an OD_{600} of 0.9 at 37°C. Cells were centrifuged at 3,200 x *g* for 10 minutes. Supernatant was discarded and pellets were frozen in -80°C.

To pull down the proteins, 1 ml of Strep-Tactin wash buffer (IBA cat # 2-1003-100) supplemented with 4 mg/ml lysozyme was added to each pellet and incubated for 10 minutes at 37°C with shaking until thawed, and then resuspended. Tubes were then transferred to ice, and the resuspended cells transferred to a FastPrep Lysing Matrix B in 2 ml tube (MP Biomedicals cat # 116911100). Samples were lysed using FastPrep bead beater for 40 seconds at 6 m/s. Tubes were centrifuged for 15 minutes at 15,000 x g. Per each pellet, 30 µl of MagStrep "Type 3" XT beads (IBA cat # 2-4090-002) were washed twice in 300 µl wash buffer (IBA cat # 2-1003-100), and the lysed cell supernatant was mixed with the beads and incubated for 30-60 minutes, rotating at 4°C. The beads were then pelleted on a magnet, washed twice with wash buffer, and purified protein was eluted from the beads in 10 µl of BXT elution buffer (IBA cat # 2-1042-025). 30 µl of samples were mixed with 10 µl of 4X Bolt™ LDS Sample Buffer (ThermoFisher cat#B0008) and a final concentration of 1mM of DTT. Samples were incubated at 75°C for 5 minutes, and then loaded to a NuPAGE™ 4 to 12%, Bis-Tris, 1.0 mm, Mini Protein Gel, 12-well (ThermoFisher cat# NP0322PK2) in 20X Bolt™ MES SDS Running Buffer (ThermoFisher cat# B0002) and run at 160V. Gels were shaken with InstantBlue® Coomassie Protein Stain (ISB1L) (ab119211) for 1 hour, followed by another hour in water. All bands shown in Fig. 3B were verified to represent the indicated protein by mass spectrometry.

Phage coinfection and hybrid isolation

50 µl overnight culture of *B. subtilis* containing DSR2 and pVip was mixed with 50 µl of phage SPR and 50 µl of either phi3T or SPbeta, each phage at a titer of 10^7 PFU/ml. Bacteria and phages were left to rest at room temperature for 10 minutes before being mixed with 5ml of premelted MMB 0.3% agar and poured over a plate containing MMB 0.5% agar. Plates were left overnight

at room temperature before being inspected for plaques. Single plaques were picked into 100 µl phage buffer (50 mM Tris-HCl pH 7.4, 100 mM $MgCl_2$, 10 mM NaCl). Hybrid phages were tested for their ability to infect DSR2-containing cells using small drop plaque assay as described above.

Sequencing and assembly of phage hybrids

High titer phage lysates (>10^7 pfu/ml) of the ancestor and isolated phage hybrids were used for DNA extraction. 500 µl of the phage lysate was treated with DNaseI (Merck cat #11284932001) added to a final concentration of 20 µg/ml and incubated at 37°C for 1 hour to remove bacterial DNA. DNA was extracted using the QIAGEN DNeasy blood and tissue kit (cat #69504) starting from the Proteinase-K treatment step to lyse the phages. Libraries were prepared for Illumina sequencing using a modified Nextera protocol as previously described [27]. Reads were de novo assembled using Spades3.14.0 [28] with the 'careful' pipeline option which reduces chances for wrong mismatches and short indels in assemblies of small genomes.

Hybrid phage alignment

Hybrid phage genomes were aligned using SnapGene Version 5.3.2. Each hybrid genome was aligned to phage SPR and areas that did not align were aligned against the other phages in the coinfection experiment in order to verify their origin and gene content.

Statistics & Reproducibility

No statistical method was used to predetermine sample size. Experiments were performed in triplicates unless stated otherwise. Randomization was used for sample injection order in mass spectrometry measurements. No data were excluded from the analyses. The experiments in Fig. 3B and Extended Data Fig.5 were repeated independently twice with similar results.

Data availability

Data that support the findings of this study are available within the Article and its Extended Data. Gene accessions appear in the Methods section of the paper. Plasmid maps of the constructs used for the experiments are attached as Supplementary Files. Source data are provided with this paper.

Acknowledgements

We thank the Sorek laboratory members for comments on the manuscript and fruitful discussion. We also thank Alexander Brandis and Tevie Mehlman from the Weizmann Life Sciences Core Facilities for targeted mass spectrometry analyses, and Alon Savidor from the Israel National Center for Personalized Medicine for protein mass spectrometry. R.S. was supported, in part, by the European Research Council (grants ERC-CoG 681203 and ERC-AdG GA 101018520), Israel Science Foundation (grant ISF 296/21), the Ernest and Bonnie Beutler Research Program of Excellence in Genomic Medicine, the Deutsche Forschungsgemeinschaft (SPP 2330, grant 464312965), the Minerva Foundation with funding from the Federal German Ministry for Education and Research, and the Knell Family Center for Microbiology. V.S. was supported by

the European Social Fund [09.3.3-LMT-K-712-01-0126] under a grant agreement with the Research Council of Lithuania (LMTLT).

Author Contributions Statement

J.G. and R.S led the study and performed all analyses and experiments unless otherwise indicated. A.L performed plaque assay experiments with the SIR2/pAgo defense system. A.B cloned and conducted plaque assays for the pVip defense system. M.Z. and V.S. provided the SIR2/pAgo defense system. S.M. and A.L. cloned and conducted plaque assays for the DSR2, DSR1 and SIR2-HerA defense systems. A.M. and G.A. assisted with sequence analysis and prediction of protein domain functions and point mutations. The manuscript was written by J.G. and R.S. All authors contributed to editing the manuscript, and support the conclusions.

Competing Interests Statement

R.S. is a scientific cofounder and advisor of BiomX and Ecophage. The other authors declare no competing interests.

Tables

Table 1. Phages used in this study

PHAGE	SOURCE	IDENTIFIER	ACCESSION
lambda(vir)	Udi Qimron		NC_001416.1
phi105	*Bacillus* Genetic Stock Center (BGSC)	BGSC (1L11)	HM072038.1
phi29	Deutsche Sammlung von Mikroorganismen und Zellkulturen (DSMZ)	DSM 5546	NC_011048.1
phi3T	*Bacillus* Genetic Stock Center (BGSC)	BGSC (1L1)	KY030782.1
SECphi17	Doron et al., 2018		LT960607.1
SECphi18	Doron et al., 2018		LT960609.1
SPbeta	*Bacillus* Genetic Stock Center (BGSC)	BGSC (1L5)	AF020713.1
SPO1	Deutsche Sammlung von Mikroorganismen und Zellkulturen (DSMZ)	BGSC (1P4)	NC_011421.1
Spp1	Deutsche Sammlung von Mikroorganismen und Zellkulturen (DSMZ)	BGSC (1P7)	NC_004166.2
SPR	*Bacillus* Genetic Stock Center (BGSC)	BGSC (1L56)	
T7	Udi Qimron		NC_001604.1
vB_EcoM-KAW1E185	Deutsche Sammlung von Mikroorganismen und Zellkulturen (DSMZ)	DSM 104099	NC_054922.1

Table 2. SIR2 containing defense systems tested in this study

SYSTEM	HOST STRAIN	NEGATIVE CONTROL	PHAGES USED FOR MS AND LIQUID GROWTH ASSAYS	PHAGES USED FOR INFECTION PLAQUE ASSAYS	TEMP. (°C)	INDUCTION
DSR2	*B. subtilis*	Empty cassette	SPR	phi29, spp1, SPR, SPbeta, phi3T, SPO1, phi105	30	Native promoter
DSR1	*B. subtilis*	Empty cassette	phi29	phi29, spp1, SPR, SPbeta, phi3T, SPO1, phi105	30	Native promoter
SIR2/ PAGO	*E. coli*	Empty pBAD	lambda(vir)	vB_EcoM-KAW1E185, lambda(vir), SECphi18, T7, SECphi17	37	0.2% arabinose
SIR2-HERA	*E. coli*	Empty vector	vB_EcoM-KAW1E185	vB_EcoM-KAW1E185, lambda(vir), SECphi18, T7, SECphi17	37	Native promoter

Fig. Legends

Fig 1. DSR2 is an abortive infection protein that causes NAD^+ depletion in infected cells. (A) Domain organization of DSR2 from *B. subtilis* 29R. Protein accession in NCBI is indicated above the gene. (B) Efficiency of plating (EOP) for three phages infecting the control *B. subtilis* BEST7003 strain (no system) or *B. subtilis* BEST7003 with DSR2 cloned from *B. subtilis* 29R. For phage SPR, EOP is also presented for two mutations in the predicted SIR2 catalytic site. Data represent plaque-forming units (PFU) per milliliter. Bar graphs represent average of three independent replicates, with individual data points overlaid. (C) Liquid culture growth of DSR2-containing *B. subtilis* and control *B. subtilis* (no system), infected by phage SPR at 30 °C. Bacteria were infected at time 0 at an MOI of 4 or 0.04. Three independent replicates are shown for each MOI, and each curve represents an individual replicate. (D-E) Concentrations of NAD^+ and ADPR in cell lysates extracted from SPR-infected cells as measured by targeted LC-MS with synthesized standards. X-axis represents minutes post infection, with zero representing non-infected cells. Cells were infected by phage SPR at a MOI of 5 at 30 °C. Bar graphs represent the average of two biological replicates, with individual data points overlaid. Colors are as in panel B.

Fig 2. Genetic exchange between phages reveal regions responsible for escape from DSR2. (A) Genome comparison of phages SPR, SPbeta and phi3T was performed using clinker [29]. Grey/black bands connect homologous genes, with shades of grey representing the % of amino acid sequence identity. (B) Schematic representation of the phage mating experiment. *B. subtilis* BEST7003 cells expressing both DSR2 and pVip are co-infected with phage SPR and SPbeta (or phi3T). Recombination between co-infecting phage genomes leads to hybrid phages that can overcome both defense systems and generate plaques. Examination of the genomes of multiple hybrids predicts genomic regions necessary to overcome defense. (C) Plaque assays with either one or two co-infecting phages. Cells expressing both DSR2 and pVip are infected either with

phage SPR (left), phage SPbeta (middle) or both phages (right). (D) Hybrid phage genomes. Each horizontal line represents the genome of a hybrid phage that can overcome DSR2. Green areas are from phage SPR, blue from SPbeta and purple from phi3T. Representative non-redundant hybrid sequences are presented out of 32 sequenced hybrids. Red rectangles outline two areas that are predicted to allow the phage to overcome DSR2 defense. Top zoom inset shows genes found in the region acquired from phi3T or SPbeta, gene outlined in red codes for DSAD1. Bottom zoom inset shows genes present in the original SPR genome, outlined gene is the tail tube protein.

Fig 3. Phage proteins that activate and inhibit DSR2. (A) DSAD1 inhibits DSR2 defense. Liquid culture growth of *B. subtilis* BEST7003 cells expressing either DSR2 alone, DSAD1 alone, or DSR2 and DSAD1, or control cells expressing neither gene, infected by phage SPR at 30 °C. Three independent replicates are shown. (B) Pulldown assays of the DSR2-DSAD1 and DSR2-tail tube complexes. DSAD1, the tail tube proteins, and control GFP were C-terminally tagged, and co-expressed with DSR2. DSR2 in this experiment was mutated (H171A) to avoid toxicity. Shown is an SDS-PAGE gel. (C) Transformation efficiencies of a vector containing the SPR tail tube protein or GFP control were measured for cells containing either WT DSR2 or two inactive DSR2 mutants. Y-axis represents the number of colony-forming units per milliliter. Bar graphs represent average of three replicates, with individual data points overlaid. (D) Liquid culture growth of *E. coli* that contains DSR2 and the tail tube gene of phage SPR, each under the control of an inducible promoter, and control *E. coli* that contains inducible GFP and DSR2 genes. Expression of both genes was induced at time 0. Three independent replicates are shown. (E-F) Concentrations of NAD^+ and ADPR in cell lysates extracted from *E. coli* co-expressing DSR2 and SPR tail tube. X-axis represents minutes post expression induction, with zero representing non-induced cells. Control cells in this experiment express RFP and DSR2. Bar graphs represent the average of two biological replicates, with individual data points overlaid. (G) A model for the mechanism of action of DSR2. Phage infection is sensed by the recognition of the phage tail tube protein through direct binding to DSR2. This triggers the enzymatic activity of the SIR2 domain to deplete the cell of NAD^+ thereby causing abortive infection. The phage anti-DSR2 protein DSAD1 inhibits DSR2 by direct binding.

Fig 4. SIR2-containing defense systems deplete NAD^+ in infected cells. (A) Domain organization of three defense systems that contain SIR2 domains. Protein accessions in NCBI are indicated. (B) Efficiency of plating for phages infecting defense-system-containing strains and control strains. SIR2-HerA and SIR2/pAgo were cloned into *E. coli* MG 1655, and DSR1 was cloned into *B. subtilis* BEST7003. Bar graphs are average of three biological replicates, with individual data points overlaid. KAW1E185 is short for vB_EcoM-KAW1E185, a T4-like phage. Asterisk marks statistically significant decrease (Student's t-test, two-sided, p-values = 0.005, 0.036, 0.025, for phages lambda (vir), KAW1E185, phi29, respectively). (C-E) Concentrations of NAD^+ in cell lysates extracted from infected cells as measured by targeted LC-MS with synthesized standards. X-axis represents minutes post infection, with zero representing non-infected cells. "No system" are control cells that contain an empty vector instead of the defense system. Bar graphs represent the average of two biological replicates, with individual data points overlaid. (F-H). Liquid culture growth of bacteria that contain the respective defense system and control bacteria that contain an empty vector (no system). Bacteria were infected at time 0 at low or high MOIs, as indicated. Three independent replicates are shown for each MOI, and each curve shows an individual replicate.

615 **References**
616
617 1. North, B. J. & Verdin, E. Protein family review Sirtuins : Sir2-related NAD-dependent
618 protein deacetylases. *Genome Biol* **5**, 224 (2004).
619 2. Imai, S., Armstrong, C. M., Kaeberlein, M. & Guarente, L. Transcriptional silencing and
620 longevity protein Sir2 is an NAD-dependent histone deacetylase. *Nature* **403**, 795–800
621 (2000).
622 3. Tanny, J. C., Dowd, G. J., Huang, J., Hilz, H. & Moazed, D. An Enzymatic Activity in the
623 Yeast Sir2 Protein that Is Essential for Gene Silencing. *Cell* **99**, 735–745 (1999).
624 4. Dang, W. & Pfizer, N. C. The controversial world of sirtuins. *Drug Discov. Today*
625 *Technol.* **12**, e9–e17 (2014).
626 5. Makarova, K. S., Wolf, Y. I., Oost, J. Van Der & Koonin, E. V. Prokaryotic homologs of
627 Argonaute proteins are predicted to function as key components of a novel system of
628 defense against mobile genetic elements. *Biol. Direct* **4**, 29 (2009).
629 6. Doron, S. *et al.* Systematic discovery of antiphage defense systems in the microbial
630 pangenome. *Science* **359**, eaar4120 (2018).
631 7. Ofir, G. *et al.* Antiviral activity of bacterial TIR domains via signaling molecules that
632 trigger cell death. *Nature* **600**, 116–120 (2021).
633 8. Gao, L. *et al.* Diverse enzymatic activities mediate antiviral immunity in prokaryotes.
634 *Science* **369**, 1077–1084 (2020).
635 9. Lopatina, A., Tal, N. & Sorek, R. Abortive Infection : Bacterial Suicide as an Antiviral
636 Immune Strategy. *Annu. Rev. Virol.* **7**, 371–384 (2020).
637 10. Kohm, K. & Hertel, R. The life cycle of SPβ and related phages. *Arch. Virol.* **166**, 2119–
638 2130 (2021).
639 11. Noyer-Weidner, M., Jentsch, S., Pawlek, B., Günthert, U. & Trautner, T. A. Restriction
640 and modification in Bacillus subtilis: DNA methylation potential of the related
641 bacteriophages Z, SPR, SP beta, phi 3T, and rho 11. *J. Virol.* **46**, 446–453 (1983).
642 12. Dragoš, A. *et al.* Pervasive prophage recombination occurs during evolution of spore-
643 forming Bacilli. *ISME J.* **15**, 1344–1358 (2021).
644 13. Bernheim, A. *et al.* Prokaryotic viperins produce diverse antiviral molecules. *Nature* **589**,
645 120–124 (2021).
646 14. Freire, D. M. *et al.* An NAD+ Phosphorylase Toxin Triggers Mycobacterium tuberculosis
647 Cell Death. *Mol. Cell* **73**, 1282-1291.e8 (2019).
648 15. Morehouse, B. R. *et al.* STING cyclic dinucleotide sensing originated in bacteria. *Nature*
649 **586**, 429–433 (2020).
650 16. Skjerning, R. B., Senissar, M., Winther, K. S., Gerdes, K. & Brodersen, D. E. The RES
651 domain toxins of RES-Xre toxin-antitoxin modules induce cell stasis by degrading NAD+.
652 *Mol. Microbiol.* **111**, 221–236 (2019).
653 17. Tang, J. Y., Bullen, N. P., Ahmad, S. & Whitney, J. C. Diverse NADase effector families
654 mediate interbacterial antagonism via the type VI secretion system. *J. Biol. Chem.* **293**,
655 1504–1514 (2018).
656 18. Tal, N. *et al.* Cyclic CMP and cyclic UMP mediate bacterial immunity against phages.
657 *Cell* **184**, 5728-5739.e16 (2021).
658 19. Millman, A. *et al.* Bacterial Retrons Function In Anti-Phage Defense. *Cell* **183**, 1551-
659 1561.e12 (2020).
660 20. Kaufmann, G. Anticodon nucleases. *Trends Biochem. Sci.* **25**, 70–74 (2000).

21. Depardieu, F. *et al.* A Eukaryotic-like Serine/Threonine Kinase Protects Staphylococci against Phages. *Cell Host Microbe* **20**, 471–481 (2016).
22. Millman, A. *et al.* An expanding arsenal of immune systems that protect bacteria from phages. Preprint at https://www.biorxiv.org/content/10.1101/2022.05.11.491447v1 (2022).
23. Cohen, D. *et al.* Cyclic GMP–AMP signalling protects bacteria against viral infection. *Nature* **574**, 691–695 (2019).
24. Overkamp, W. *et al.* Benchmarking various green fluorescent protein variants in Bacillus subtilis, Streptococcus pneumoniae, and Lactococcus lactis for live cell imaging. *Appl. Environ. Microbiol.* **79**, 6481–6490 (2013).
25. Wilson, G. A. & Bott, K. F. Nutritional Factors Influencing the Development of Competence in the Bacillus subtilis Transformation System. *J. Bacteriol.* **95**, 1439–1449 (1968).
26. Mazzocco A, Waddell TE, Lingohr E, J. R. Enumeration of bacteriophages using the small drop plaque assay system. *Methods Mol. Biol.* **501**, 81–85 (2009).
27. Baym, M. *et al.* Inexpensive multiplexed library preparation for megabase-sized genomes. *PLoS One* **10**, e0128036 (2015).
28. Prjibelski, A., Antipov, D., Meleshko, D., Lapidus, A. & Korobeynikov, A. Using SPAdes De Novo Assembler. *Curr. Protoc. Bioinforma.* **70**, 1–29 (2020).
29. Gilchrist, C. L. M. & Chooi, Y.-H. Clinker & Clustermap.Js: Automatic Generation of Gene Cluster Comparison Figures. *Bioinformatics* **37**, 2473–2475 (2021).
30. Gabler, F. *et al.* Protein Sequence Analysis Using the MPI Bioinformatics Toolkit. *Curr. Protoc. Bioinforma.* **72**, 1–30 (2020).
31. Zaremba, M. *et al.* Sir2-domain associated short prokaryotic Argonautes provide defence against invading mobile genetic elements through NAD+ depletion. Preprint at https://www.biorxiv.org/content/10.1101/2021.12.14.472599v1 (2021).
32. Altschul, S. F. *et al.* Gapped BLAST and PSI-BLAST: A new generation of protein database search programs. *Nucleic Acids Res.* **25**, 3389–3402 (1997).

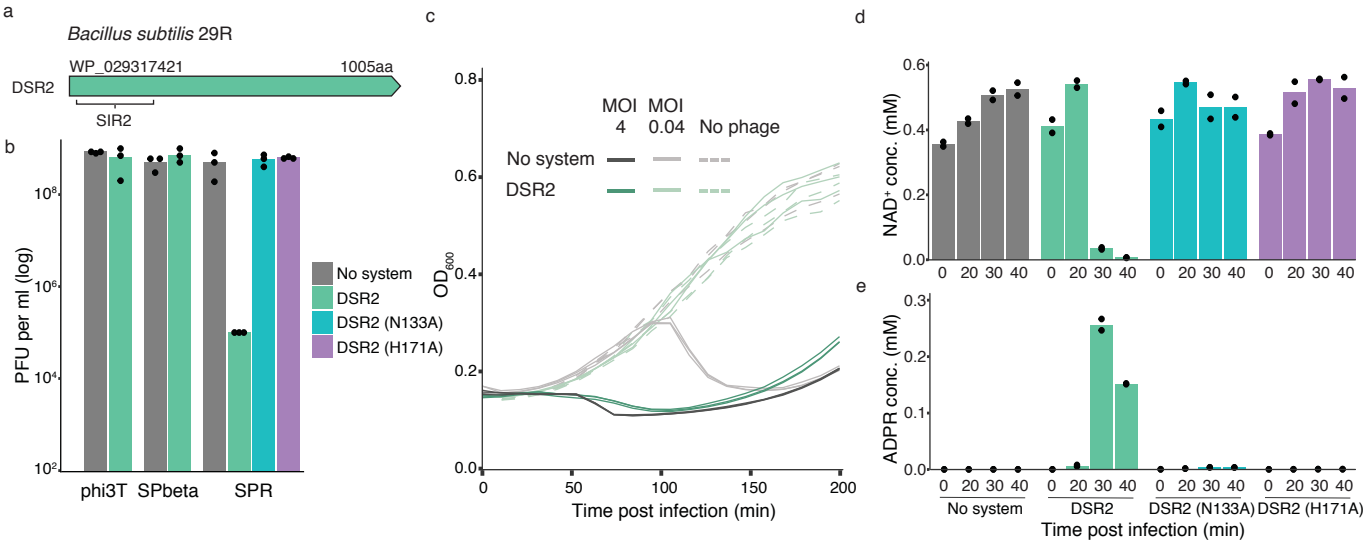
a
Bacillus subtilis 29R
WP_029317421
1005aa
DSR2
SIR2
b
PFU per ml (log)
phi3T
SPbeta
SPR
No system
DSR2
DSR2 (N133A)
DSR2 (H171A)
c
MOI 4
MOI 0.04
No phage
No system
DSR2
OD600
Time post infection (min)
d
NAD+ conc. (mM)
e
ADPR conc. (mM)
No system
DSR2
DSR2 (N133A)
DSR2 (H171A)
Time post infection (min)

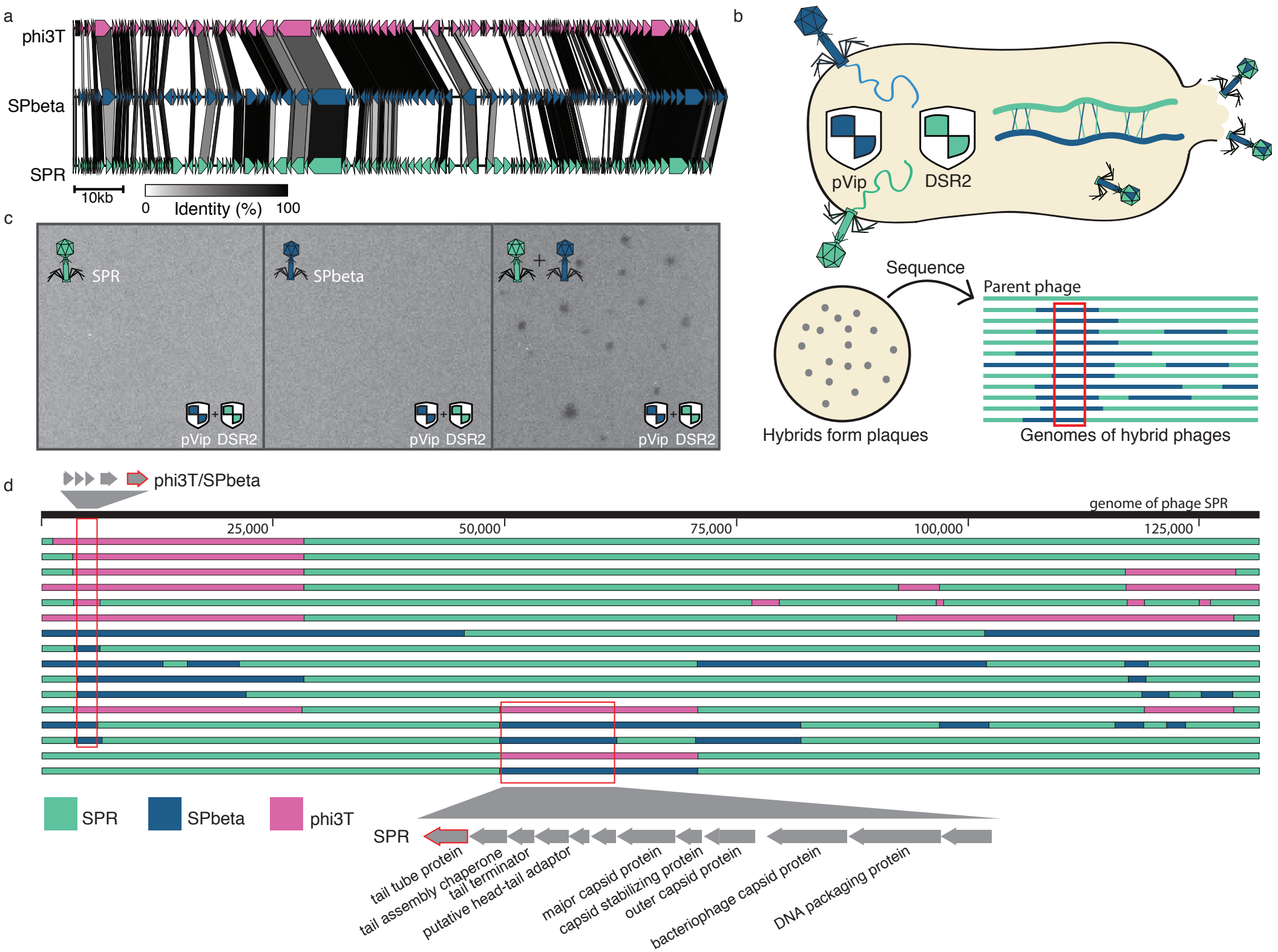
a
phi3T
SPbeta
SPR
10kb
0
Identity (%)
100
b
pVip
DSR2
Sequence
Parent phage
Hybrids form plaques
Genomes of hybrid phages
c
SPR
SPbeta
pVip DSR2
pVip DSR2
pVip DSR2
d
phi3T/SPbeta
genome of phage SPR
25,000
50,000
75,000
100,000
125,000
SPR
SPbeta
phi3T
SPR
tail tube protein
tail assembly chaperone
tail terminator
putative head-tail adaptor
major capsid protein
capsid stabilizing protein
outer capsid protein
bacteriophage capsid protein
DNA packaging protein

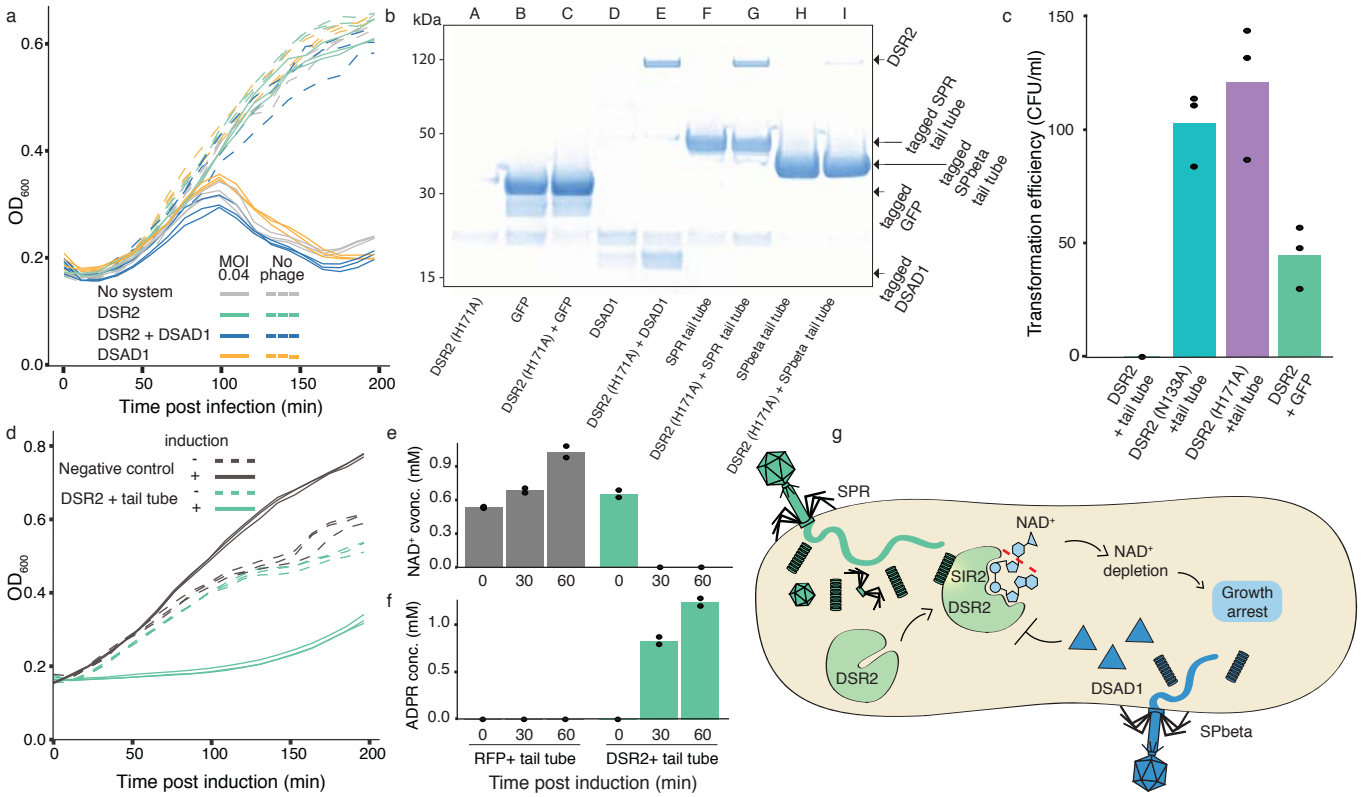
a
b
c
d
e
f
g
OD600
Time post infection (min)
MOI 0.04
No phage
No system
DSR2
DSR2 + DSAD1
DSAD1
kDa
DSR2
tagged SPR tail tube
tagged SPbeta tail tube
tagged GFP
tagged DSAD1
DSR2 (H171A)
GFP
DSR2 (H171A) + GFP
DSAD1
DSR2 (H171A) + DSAD1
SPR tail tube
DSR2 (H171A) + SPR tail tube
SPbeta tail tube
DSR2 (H171A) + SPbeta tail tube
Transformation efficiency (CFU/ml)
DSR2 + tail tube
DSR2 (N133A) +tail tube
DSR2 (H171A) +tail tube
DSR2 + GFP
induction
Negative control
DSR2 + tail tube
Time post induction (min)
NAD+ cvonc. (mM)
ADPR conc. (mM)
RFP+ tail tube
DSR2+ tail tube
Time post induction (min)
SPR
NAD+
NAD+ depletion
SIR2
DSR2
DSR2
Growth arrest
DSAD1
SPbeta

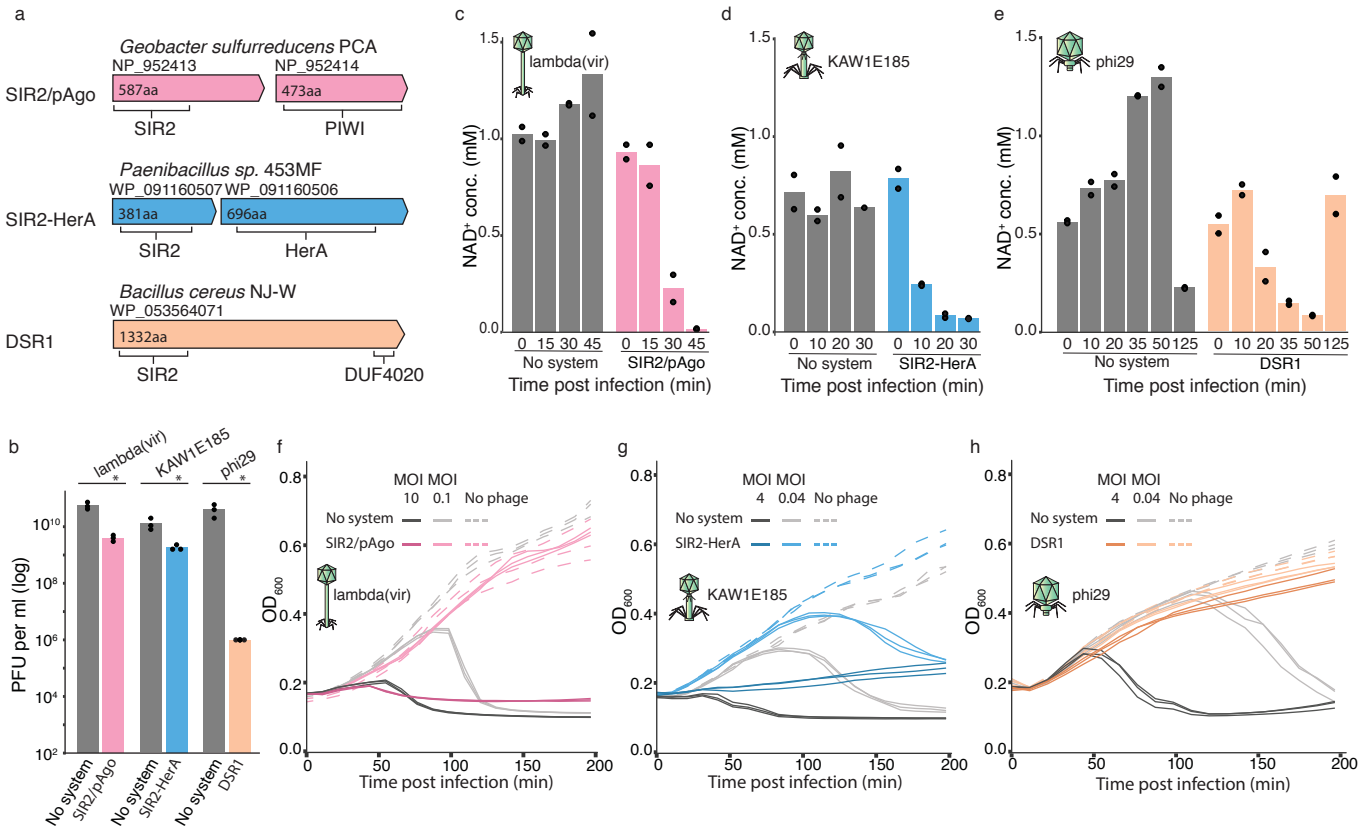
a
Geobacter sulfurreducens PCA
NP_952413
NP_952414
SIR2/pAgo
587aa
473aa
SIR2
PIWI
Paenibacillus sp. 453MF
WP_091160507 WP_091160506
SIR2-HerA
381aa
696aa
SIR2
HerA
Bacillus cereus NJ-W
WP_053564071
DSR1
1332aa
SIR2
DUF4020
b
lambda(vir)
KAW1E185
phi29
PFU per ml (log)
No system
SIR2/pAgo
SIR2-HerA
DSR1
c
lambda(vir)
NAD+ conc. (mM)
No system
SIR2/pAgo
Time post infection (min)
d
KAW1E185
No system
SIR2-HerA
Time post infection (min)
e
phi29
No system
DSR1
Time post infection (min)
f
MOI MOI
10 0.1 No phage
No system
SIR2/pAgo
lambda(vir)
OD600
Time post infection (min)
g
MOI MOI
4 0.04 No phage
No system
SIR2-HerA
KAW1E185
Time post infection (min)
h
MOI MOI
4 0.04 No phage
No system
DSR1
phi29
Time post infection (min)

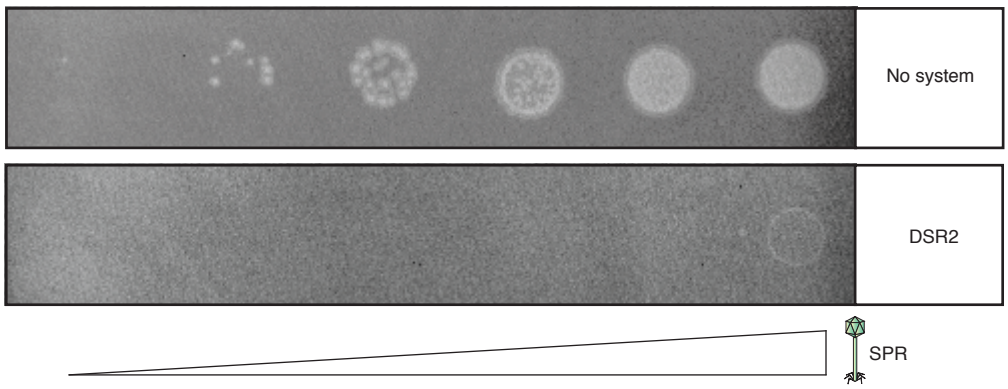
No system
DSR2
SPR

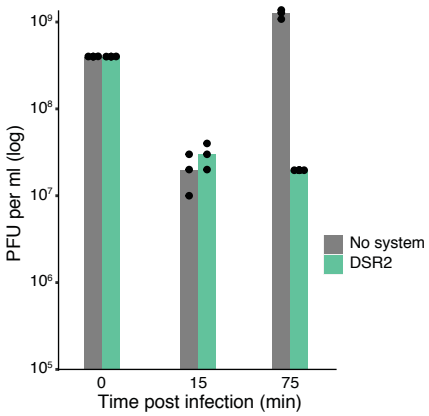
10^9
10^8
10^7
10^6
10^5
PFU per ml (log)
0
15
75
Time post infection (min)
No system
DSR2

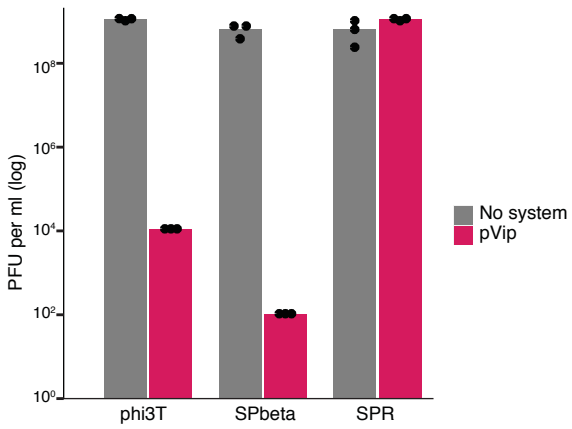
PFU per ml (log)
10^8
10^6
10^4
10^2
10^0
phi3T
SPbeta
SPR
No system
pVip

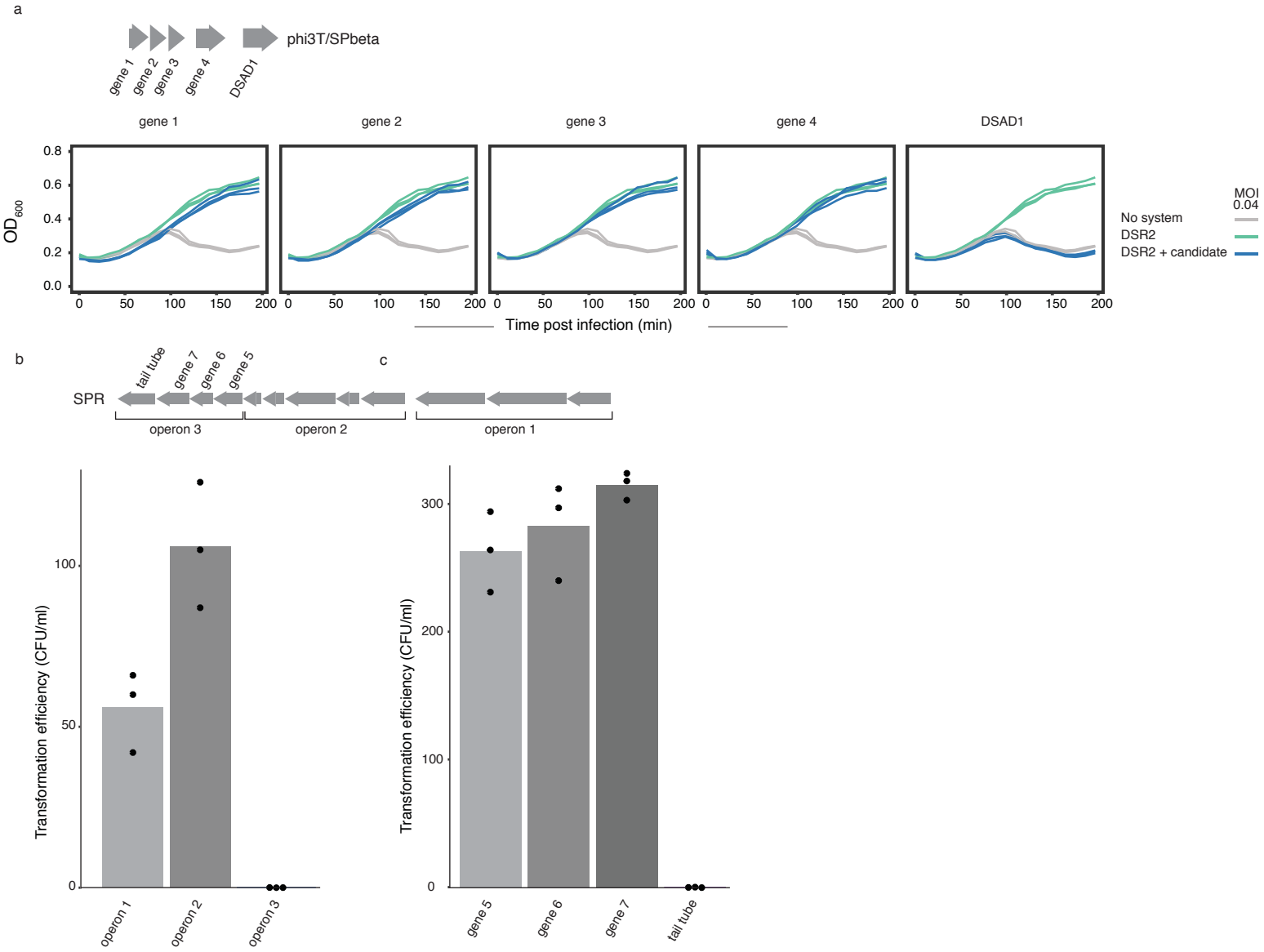
a
phi3T/SPbeta
gene 1
gene 2
gene 3
gene 4
DSAD1
gene 1
gene 2
gene 3
gene 4
DSAD1
OD600
0.8
0.6
0.4
0.2
0.0
0
50
100
150
200
Time post infection (min)
MOI
0.04
No system
DSR2
DSR2 + candidate
b
c
SPR
tail tube
gene 7
gene 6
gene 5
operon 3
operon 2
operon 1
Transformation efficiency (CFU/ml)
100
50
0
operon 1
operon 2
operon 3
Transformation efficiency (CFU/ml)
300
200
100
0
gene 5
gene 6
gene 7
tail tube

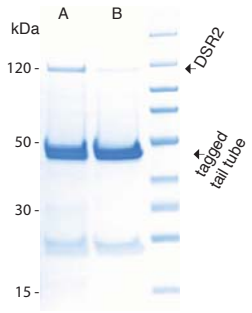
A
B
kDa
120 -
50 -
30 -
15 -
DSR2
tagged
tail tube

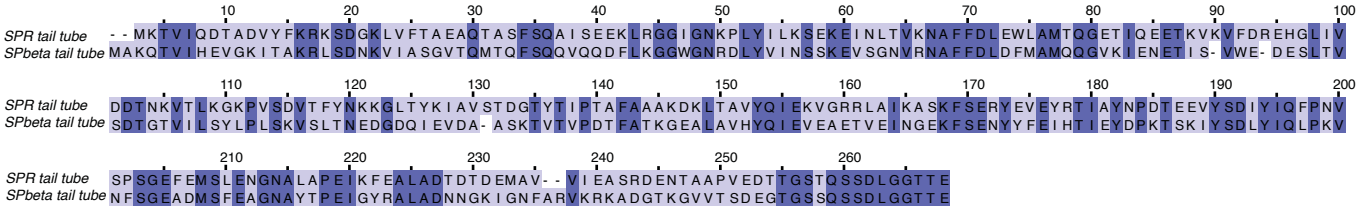
10 20 30 40 50 60 70 80 90 100
SPR tail tube --MKTVIQDTADVYFKRKSDGKLVFTAEAQTASFSQAISEEKLRGGIGNKPLYILKSEKEINLTVKNAFFDLEWLAMTQGETIQEETKVKVFDREHGLIV
SPbeta tail tube MAKQTVIHEVGKITAKRLSDNKVIASGVTQMTQFSQQVQQDFLKGGWGNRDLYVINSSKEVSGNVRNAFFDLDFMAMQQGVKIENETIS-VWE-DESLTV
110 120 130 140 150 160 170 180 190 200
SPR tail tube DDTNKVTLKGKPVSDVTFYNKKGLTYKIAVSTDGTYTIPTAFAAAKDKLTAVYQIEKVGRRLAIKASKFSERYEVEYRTIAYNPDTEEVYSDIYIQFPNV
SPbeta tail tube SDTGTVILSYLPLSKVSLTNEDGDQIEVDA-ASKTVTVPDTFATKGEALAVHYQIEVEAETVEINGEKFSENYYFEIHTIEYDPKTSKIYSDLYIQLPKV
210 220 230 240 250 260
SPR tail tube SPSGEFEMSLENGNALAPEIKFEALADTDTDEMAV--VIEASRDENTAAPVEDTTGSTQSSDLGGTTE
SPbeta tail tube NFSGEADMSFEAGNAYTPEIGYRALADNNGKIGNFARVKRKADGTKGVVTSDEGTGSSQSSDLGGTTE

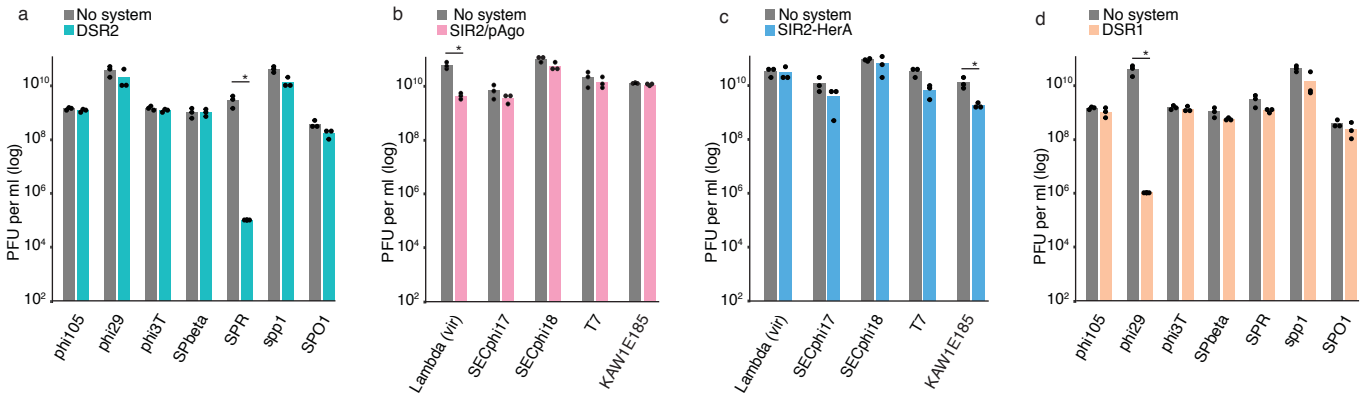
a
No system
DSR2
b
No system
SIR2/pAgo
c
No system
SIR2-HerA
d
No system
DSR1
PFU per ml (log)
10^{10}
10^{8}
10^{6}
10^{4}
10^{2}
*
phi105
phi29
phi3T
SPbeta
SPR
spp1
SPO1
Lambda (vir)
SECphi17
SECphi18
T7
KAW1E185

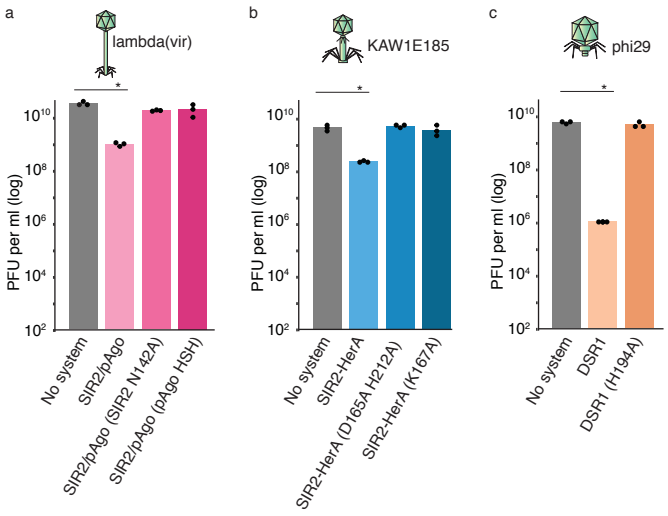
a
lambda(vir)
*
PFU per ml (log)
10^{10}
10^{8}
10^{6}
10^{4}
10^{2}
No system
SIR2/pAgo
SIR2/pAgo (SIR2 N142A)
SIR2/pAgo (pAgo HSH)
b
KAW1E185
*
PFU per ml (log)
10^{10}
10^{8}
10^{6}
10^{4}
10^{2}
No system
SIR2-HerA
SIR2-HerA (D165A H212A)
SIR2-HerA (K167A)
c
phi29
*
PFU per ml (log)
10^{10}
10^{8}
10^{6}
10^{4}
10^{2}
No system
DSR1
DSR1 (H194A)

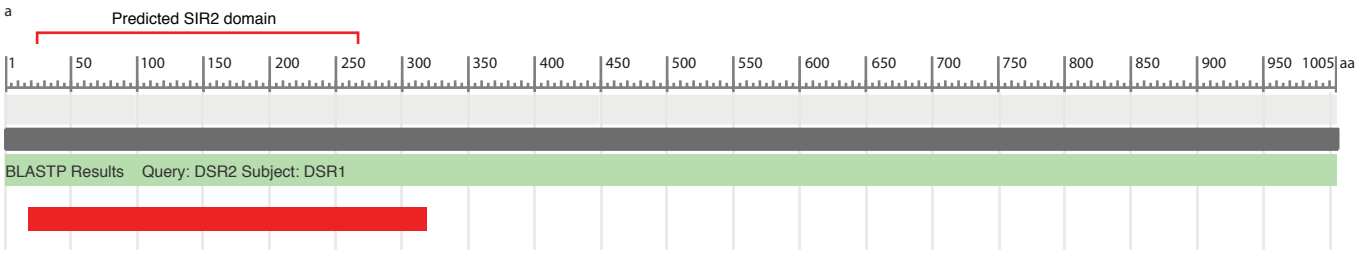
a
Predicted SIR2 domain
1
50
100
150
200
250
300
350
400
450
500
550
600
650
700
750
800
850
900
950
1005
aa
BLASTP Results Query: DSR2 Subject: DSR1

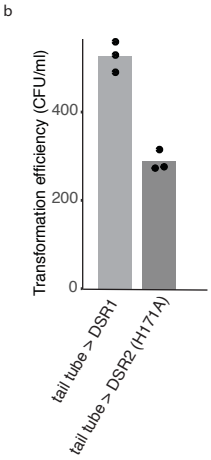
b
Transformation efficiency (CFU/ml)
400
200
0
tail tube > DSR1
tail tube > DSR2 (H171A)

JG1	ggatccaaactcgagtaaggatctcca
JG2	agtagttcctccttatgtactagtagttacatttattgtac
JG3	aactactagtacataaggaggaactactatgaacatcaagaccattgtgatcaactggc
JG4	gcctggagatccttactcgagtttggatccttagtcgtcagacaagtcggtaaagc
JG13	taataatgagcactagtcaaggtcggc
JG14	gtttgtcctccttattagttaatcagctagc
JG81	gcaatagttacccttattatcaagataag
JG82	cttgataataagggtaactattgcgatcctagaagcttatcgaattccttattaacgt
JG83	cttaggagcgtacattactaagcaaaacccgtaccctagg
JG134	gattaactaataaggaggacaaacatggacagtagagaacaaattgattggac
JG142	accttgactagtgctcattattattcagttgttccgccaagatctga
JG143	gattaactaataaggaggacaaacatgaaaacagttattcaagatacagctgacgtttattttaaacgaaaat
JG183	accttgactagtgctcattatcaatcaagtatcttatttttggctttatatcgatttcat
JG184	gattaactaataaggaggacaaacttgattaagacgttgatttcatttagtgggataaact
JG185	accttgactagtgctcattatcacaataaagttttatcaatgttattgtctgatttaatttcaaagt
JG186	gattaactaataaggaggacaaacatgaaggaaagtctcatgatttatttcaatattgaaaact
JG187	accttgactagtgctcattatcatgttttattgtggcagatattaatatattccttcagg
JG188	gattaactaataaggaggacaaacttggaggaaagatacctgattgttacagc
JG189	accttgactagtgctcattatcattgaaataatcctccccaaatcactcc
JG216	tatcataagcagttgtaattacatgtgctggg
JG217	gcacatgtaattacaactgcttatgataatttgattgatactgc
JG220	taaaggttgctggggattttagaaagggcttt
JG221	aaatccccagcaacctttagtaaataccttgatga
JG249	cttactcgagtttggatccttattcagttgttccgccaagatctgagc
JG250	gatcttttaagaaggagatatacatatgaaaacagttattcaagatacagctgacg
JG259	gatcttttaagaaggagatatacatatggtgaaggtggatttggaaagtaaaag
JG260	cttactcgagtttggatccttagataaagtagttcattaaaatttccaaatacctcttatcatttgag
MZ325	gctgatggtctcgcatggatgtcttaactgacaatgagttttac
MZ326	tgatgctcgagcataaaaaaccgataatcatatatttcgttaac
JG346	gattaactaataaggaggacaaacatgattgaaatttttaaagatacaggagctacc
JG347	accttgactagtgctcattattaatctagataaacaac
JG366	gatcttttaagaaggagatatacatatgtcaaaaggagaagaacttttttacaggtg
JG367	cttactcgagtttggatccttacttttcaaactgaggatgcgaccac
JG406	ggatccaaactcgagtaaggatctcca
JG407	gttgacacagggaacggct
JG408	gatcttttaagaaggagatatacatatgaaaacagttattcaagatacagctgacg
JG409	cgttccctgtgtcaacttcagttgttccgccaagatctgag
JG410	gatcttttaagaaggagatatacatatgattgaaatttttaaagatacaggagctaccca
JG411	cgttccctgtgtcaacatctagataaacaacttcttttacaattggaaatggac
JG412	gttgacacagggaacggct
JG421	gatcttttaagaaggagatatacatatggcaaaacaaacagtaatccatgaag
JG422	cgttccctgtgtcaacttcagttgttccgccaagatctgag
JG427	ttttttctgcaggtcgacaagct

JG428	atgtatatctccttcattaaatctagaggatcccc
JG429	tagatttaatgaaggagatatacatatgattgaaatttttaaagatacaggagctaccca
JG430	gtcgacctgcagaaaaaattaatctagataaacaacttcttttacaattggaaatggac
JG431	accttgactagtgctcattatcataagccagagggcgtacc
JG432	gattaactaataaggaggacaaacatggtgggtcggaaacctaaagaaaaagaaaaact
JG433	accttgactagtgctcattatcactcgaaattattggttttaagcttgct
JG434	gattaactaataaggaggacaaacatgccgctgtgtgtagaatttattga
JG435	accttgactagtgctcattattattcagttgttccgccaagatctga
JG436	gattaactaataaggaggacaaacatgtcaatagattggtacctttcttcctcc
JG437	accttgactagtgctcattatcatgccatttcaccaactttctttttggc
JG438	gattaactaataaggaggacaaacatgtcaatagattggtacctttcttcctcc
JG439	accttgactagtgctcattatcatttcatcgccccaaaggtatatattaatttatatcc
JG440	gattaactaataaggaggacaaacatgagcatgactgttgaacagatgac
JG441	accttgactagtgctcattactatgcgctgcctttaccaaaac
JG442	gattaactaataaggaggacaaacatgattgatagtgaattctttataaccggtgaac
JG463	tttcacaaccgcctttgatgatgtcatag
JG464	acaactttggtctggttc
JG496	aattcatattgctggtagtgtaaaaaaagaag
JG497	acattcccatttttagttc
JG498	acaaattatgccttgctaatggag
JG499	tgtaaaaatttccacctgg
JG500	ttggaagttggctggctcaataaactg
JG501	agtttagaccatcttgatg
JG502	aggctcaggggcatccactacc
JG503	gttgaccccaaaactgcg
OGO603	ttagtaatgtacgctcctaagaag

Multiple phage resistance systems inhibit infection via SIR2-dependent NAD^+ depletion

Jeremy Garb[1], Anna Lopatina[1,‡], Aude Bernheim[1,#], Mindaugas Zaremba[2], Virginijus Siksnys[2], Sarah Melamed[1], Azita Leavitt[1], Adi Millman[1], Gil Amitai[1], Rotem Sorek[1,*]

[1]Department of Molecular Genetics, Weizmann Institute of Science, Rehovot 7610001, Israel

[2] Institute of Biotechnology, Life Sciences Center, Vilnius University, Sauletekio al. 7, LT-10257 Vilnius, Lithuania

[‡] Present address: Division of Microbial Ecology, Department of Microbiology and Ecosystem Science, Center for Microbiology and Environmental Systems Science, University of Vienna, Vienna, Austria.

[#] Present address: SEED, U1284, INSERM, Université Paris Cité, Paris, France.

[*]correspondence: rotem.sorek@weizmann.ac.il

Abstract

Defense-associated sirtuins (DSR) comprise a family of proteins that defend bacteria from phage infection via an unknown mechanism. These proteins are common in bacteria and harbor an N-terminal sirtuin (SIR2) domain. In this study we report that DSR proteins degrade nicotinamide adenine dinucleotide (NAD^+) during infection, depleting the cell of this essential molecule and aborting phage propagation. Our data show that one of these proteins, DSR2, directly identifies phage tail tube proteins and then becomes an active NADase in *Bacillus subtilis*. Using a phage mating methodology that promotes genetic exchange between pairs of DSR2-sensitive and DSR2–resistant phages, we further show that some phages express anti-DSR2 proteins that bind and repress DSR2. Finally, we demonstrate that the SIR2 domain serves as an effector NADase in a diverse set of phage defense systems outside the DSR family. Our results establish the general role of SIR2 domains in bacterial immunity against phages.

Introduction

SIR2-domain proteins, or sirtuins, are found in organisms ranging from bacteria to humans. These proteins have been widely studied in yeast and mammals, where they were shown to regulate transcription repression, recombination, DNA repair and cell cycle processes [1]. In eukaryotes, SIR2 domains were shown to possess enzymatic activities, and function either as protein deacetylases or ADP ribosyltransferases [2,3]. In both cases, the SIR2 domain utilizes nicotinamide adenine dinucleotide (NAD^+) as a cofactor for the enzymatic reaction [4].

In bacteria, SIR2 domains were recently shown to participate in defense systems that protect against phages. These domains are associated with multiple different defense systems, including prokaryotic argonautes (pAgo) [5], Thoeris [6,7], AVAST, DSR, and additional systems [8]. It was recently shown that the SIR2 domain in the Thoeris defense system is an NADase responsible for depleting NAD^+ from the cell once phage infection has been sensed [7]. However, it is currently unknown whether SIR2 domains in other defense systems perform a similar function, or whether they have other roles in phage defense.

Results

DSR2 defends against phage SPR via abortive infection

To study the role of SIR2 domains in bacterial anti-phage defense, we began by focusing on DSR2, a minimal defense system that includes a single protein with an N-terminal SIR2 domain and no additional identifiable domains (Fig. 1A). The DSR2 gene family was recently identified based on a screen for genes commonly found in bacterial anti-phage defense islands [8]. We cloned the DSR2 gene from *Bacillus subtilis* 29R, under the control of its native promoter, into the genome of *B. subtilis* BEST7003 which naturally lacks this gene, and challenged the DSR2-containing strain with a set of phages from the SPbeta family. We found that DSR2 protected *B. subtilis* against phage SPR, reducing plating efficiency by four orders of magnitude (Fig. 1B, Extended Data Fig.1). Point mutations in residues N133 and H171 in DSR2, both of which predicted to disable the active site of the SIR2 domain, abolished defense, suggesting that the enzymatic activity of SIR2 is essential for DSR2 defense (Fig. 1B).

We next tested whether DSR2 defends via abortive infection, a process that involves premature death or growth arrest of the infected cell, preventing phage replication and spread to nearby cells [9]. When infected in liquid media, DSR2-containing bacterial cultures collapsed if the culture was infected by phage in high multiplicity of infection (MOI), similar to DSR2-lacking cells (Fig. 1C). However, despite collapsing the culture, phages were not able to replicate on DSR2-containing cells (Extended Data Fig.2). In low MOI infection, DSR2-lacking control cultures collapsed but DSR2-containing bacteria survived (Fig. 1C). This phenotype is a hallmark of abortive infection, in which infected bacteria that contain the defense system do not survive but also do not produce phage progeny [9].

DSR2 depletes NAD^+ upon phage infection

To ask whether DSR2 manipulates the NAD^+ content of the cell during phage infection, we used mass spectrometry to monitor NAD^+ levels in infected cells at various time points following initial

infection. When DSR2-containing cells were infected by phage SPR, cellular NAD^+ decreased sharply between 20 and 30 minutes from the onset of infection (Fig. 1D). NAD^+ levels did not change in cells in which the SIR2 active site was mutated, or in DSR2-lacking control cells, suggesting that the SIR2 domain is responsible for the observed NAD^+ depletion (Fig. 1D). In parallel with NAD^+ depletion, we observed accumulation of the product of NAD^+ cleavage, ADP-ribose (ADPR) (Fig. 1E). These results demonstrate that DSR2 is an abortive infection protein that causes NAD^+ depletion in infected cells.

DSR2 strongly protected *B. subtilis* cells against SPR, a phage belonging to the SPbeta group of phages [10] (Fig. 1B, Extended Data Fig.1). However, the defense gene failed to protect against phages phi3T and SPbeta, although both these phages belong to the same phage group as SPR (Fig. 1B). This observation suggests that phages phi3T and SPbeta either encode genes that inhibit DSR2, or lack genes that are recognized by DSR2 and trigger its NADase activity. The phages SPR, phi3T and SPbeta all share substantial genomic regions with high sequence homology (Fig. 2A). We therefore reasoned that co-infecting cells with two phages, either SPR and phi3T, or SPR and SPbeta, may result in recombination-mediated genetic exchange between the phages, which would enable pinpointing genes that allow escape from DSR2 defense when acquired by SPR (Fig. 2B). Such crossing techniques were previously successful in pinpointing genetic phenotypes in phages [11,12].

To generate a bacterial host that would select for such genetic exchange events, we cloned into DSR2-containing cells an additional defense protein, a prokaryotic viperin homolog (pVip) from *Fibrobacter* sp. UWT3 [13]. The pVip protein, when expressed alone in *B. subtilis*, protected it from phi3T and SPbeta but not from SPR, a defense profile which is opposite to that of the DSR2 profile in terms of the affected phages (Extended Data Fig.3). Accordingly, none of the three SPbeta-group phages could form plaques on the strain that expressed both defensive genes. However, when simultaneously infecting the double defense strain with SPR and either phi3T or SPbeta, plaque forming hybrids were readily obtained, indicating that these hybrid phages recombined and acquired a combination of genes enabling them to escape both DSR2 and pVip (Fig. 2C).

A phage-encoded anti-DSR2 protein

We isolated and sequenced 32 such hybrid phages, assembled their genomes, and compared these genomes to the genome of the parent SPR phage (Fig. 2D; Supplementary File 1). This led to the identification of two genomic segments that were repeatedly acquired by SPR phages. Acquisition of either of these segments from a genome of a co-infecting phage rendered SPR resistant to DSR2 (Fig. 2D). The first segment included five small genes of unknown function that are present in phages phi3T and SPbeta but not in the wild type SPR phage, and we therefore tested whether any of these genes was capable of inhibiting DSR2. One of the genes, when co-expressed with DSR2, rendered DSR2 inactive, suggesting that this phage gene encodes an anti-DSR2 protein (Fig. 3A). The other four genes in the segment did not inhibit DSR2 defense (Extended Data Fig.4A). The DSR2-inhibiting protein, which we named DSAD1 (DSR Anti Defense 1), is 120aa long and has no identifiable sequence homology to proteins of known function. Co-expression of DSR2 and tagged DSAD1, followed by pulldown assays, showed direct interaction between the two proteins (Fig. 3B). These results indicate that DSAD1 is a phage protein that binds and inhibits DSR2.

DSR2 is activated by phage tail tube protein

We next examined the second genomic segment that, when acquired, allowed phage hybrids to escape DSR2. In the parent SPR phage, this region spans three operons encoding a set of phage structural proteins, including capsid and tail proteins. Hybrid phages in which the original genes were replaced by their homologs from SPbeta or phi3T become resistant to DSR2 (Fig. 2D). We hypothesized that one of the structural proteins in phage SPR is recognized by DSR2 to activate its defense, and when this protein is replaced by its homolog from another phage, recognition no longer occurs. To test this hypothesis, we attempted to clone each of the three operons found in the original DNA segment in SPR into *B. subtilis* cells that also express DSR2. One of these operons could not be cloned into DSR2-expressing cells, and we then repeated the cloning attempt for each of the genes in the operon. One of these genes, encoding a tail tube protein, could not be cloned into DSR2-expressing cells but was readily cloned into cells in which the DSR2 active site was mutated (Fig. 3C, Extended Data Fig.4B-C).

To further test if co-expression of DSR2 and the SPR tail tube protein is toxic to bacteria, we cloned each of these genes under an inducible promoter within *E. coli* cells. In support of our hypothesis, growth was rapidly arrested in cells in which the expression of both genes was induced (Fig. 3D), and these cells became depleted of NAD^+ (Fig. 3E, 3F). Furthermore, pulldown assays with tagged proteins showed that DSR2 directly binds the tail tube protein of phage SPR (Fig. 3B). The tail tube protein was not able to pull down DSR2 when DSAD1 was coexpressed in the same cells, suggesting that the tail tube protein and DSAD1 are competitive binders for DSR2 (Extended Data Fig.5). These results demonstrate that the tail tube protein of phage SPR is directly recognized by the defense protein DSR2, and that this recognition triggers the NADase activity of DSR2 and results in growth arrest (Fig. 3G).

The original tail tube protein of phage SPR is substantially divergent from its counterparts from phages SPbeta or phi3T, sharing only ~40% amino acid sequence identity with these proteins (Extended Data Fig.6). This divergence explains why the replacement of the original SPR protein with its SPbeta homolog renders the hybrid phage resistant to DSR2. In support of this, the tail tube protein of phage SPbeta showed much weaker ability to pull down DSR2 as compared to the tail tube counterpart from phage SPR (Fig. 3B). Presumably, the evolutionary pressure imposed by DSR2 and other bacterial defense systems that recognize tail tube proteins has led to the observed diversification in these proteins in phages of the SPbeta group.

Various defense systems with SIR2 domains deplete NAD^+ upon infection

Our results show that DSR2 exerts its defensive activity by depleting NAD^+ from infected cells. NADase activity was also recently described in the Thoeris defense system, in which a small molecule signal activates a SIR2-encoding effector to deplete NAD^+ once phage infection has been recognized [7]. To test if NAD^+ depletion is a general activity of SIR2 domains in bacterial defense systems, we examined three additional defense systems that contain a SIR2 domain (Fig. 4A). These systems included a two-gene system that encodes, in addition to the SIR2 domain, also a prokaryotic argonaute homolog (pAgo), a two-gene system that encodes a HerA-like DNA translocase [8], and a single SIR2-domain protein called DSR1 [8] (Fig. 4A). DSR1 was cloned into *B. subtilis* BEST7003, while the other two systems were cloned into an *E. coli* host. Consistent with our hypothesis, these systems defended against multiple different phages (Fig. 4B, Extended Data Fig.7), and NAD^+ depletion was observed in each case (Fig. 4C-E). Mutations inactivating

the HerA-like DNA translocase or the pAgo protein abolished defense, indicating that these two proteins also participate in the defensive function (Extended Data Fig.8). Liquid infection with high and low MOIs showed a phenotype consistent with abortive infection for the SIR2/pAgo and the SIR2-HerA systems (Fig. 4F-G). However, the DSR1 protein seems to inhibit the replication of phage phi29 without arresting the growth of the bacterial cells, and depletion of NAD^+ was only transient (Fig. 4E, 4H). Together, these results demonstrate a general role of SIR2 domains as NAD^+ depleting effectors in bacterial defense against phage.

Discussion

Our data suggest that NAD^+ depletion is a canonical function for SIR2 domains within bacterial defense systems. We show that four anti-phage defense systems, all containing SIR2 domains but otherwise comprising different architectures, deplete NAD^+ in response to phage infection. Specifically, in the case of DSR2, we show that this protein recognizes newly translated phage tail tube proteins to become an active NADase. Phages of the SPbeta family have at least two versions of the tail tube protein, and only certain alleles are strongly recognized by DSR2. In addition, we found that some phages in this family carry a small protein, DSAD1, which binds and inactivates DSR2.

NAD^+ depletion was previously shown to be toxic to bacterial cells [14–17], and it was recently demonstrated in the Thoeris, CBASS and Pycsar systems that defense involving NAD^+ depletion during phage infection is associated with an eventual cell death [7,15,18]. Indeed, in three out of the four SIR2-containing systems that we studied, growth arrest or death of the bacterial host was observed in response to phage infection. However, DSR1 protection from phage phi29 did not involve culture collapse (Fig. 4H). Furthermore, our data show that the NAD^+ levels in cells containing DSR1 recovered after the initial depletion (Fig. 4E). It is possible that in some cases, reversible reduction of NAD^+ to low but not zero levels may be enough to interfere with phage replication while still allowing cell growth. Alternatively, lowered levels of NAD^+ might have different outcomes for the infected cell depending on additional components derived from the infecting phage.

The molecular signatures recognized by abortive infection defense systems as an indication for phage infection have been notoriously challenging to discover. In a minority of cases where the trigger was discovered, it was shown that some systems "guard" an immunity hub in the cell, and become triggered when the phage tampers with the immunity complex [19,20]. In other cases, a specific protein expressed by the phage during infection forms the trigger for system activation, as shown for the *Staphylococcus* Stk2 abortive infection kinase [21], and also as we show for DSR2 in the current study. However, the SPR tail tube protein that activates DSR2 does not activate DSR1, suggesting that these two proteins recognize different molecular signatures (Extended Data Fig.9). The mechanisms by which phages activate, and potentially inhibit, the other three SIR2-domain-containing systems described in this study remains to be elucidated by future studies.

The arsenal of defense mechanisms known to protect bacteria against phage has recently been substantially expanded following the discovery of dozens of new anti-phage defense systems [6,8,22]. While the mechanism of defense was deciphered for some of these systems [7,13,18,23], in many cases it is not known what molecular patterns of the phage trigger these systems to become active. In the

current study we used a "phage mating" technique, which was previously successfully used in other studies [11,12], to promote genetic exchange between phages that are sensitive to the defense system and phages that can overcome it. Genome analyses of hybrid phages enabled us to pinpoint the exact phage proteins that activate or repress DSR2. We believe that the phage mating approach should be a useful tool for other studies attempting to identify phage triggers of bacterial defense systems.

Methods

Bacterial strains and phages

B. subtilis strain BEST7003 (obtained from I. Mitsuhiro at Keio University, Japan) was grown in MMB (LB + 0.1 mM MnCl2 + 5 mM $MgCl_2$, with or without 0.5% agar) at 30 °C. Whenever applicable, media were supplemented with spectinomycin (100 µg/ml) and chloramphenicol (5 µg/ml), to ensure selection of transformed and integrated cells. *E. coli* strain MG1655 (ATCC 47076) was grown in MMB at 37 °C. Whenever applicable, media were supplemented with ampicillin (100 µg/ml) or chloramphenicol (30 µg/ml) or kanamycin (50 µg/ml), to ensure the maintenance of plasmids. Phages used in this study are listed in Table 1.

Plasmid and strain construction

Details on defense systems analyzed in this study are summarized in Table 2, and sequences of primers used in this study are in Supplementary Table S3. Defense systems DSR1, DSR2, and SIR2-HerA were synthesized by Genscript Corp. and cloned into the pSG1 plasmid [6] together with their native promoters. A whole operon of the SIR2/pAgo system, composed of the genes encoding the SIR2 (GSU1360, NP_952413.1) and pAgo (GSU1361, NP_952414.1) proteins, was amplified by PCR using the oligonucleotides MZ239 and MZ240, respectively, from the genomic DNA of *Geobacter sulfurreducens* Caccavo (LGC Standards cat #51573D-5). The resulting DNA fragment was digested by Eco31I (ThermoFisher cat #FD0293) and XhoI (ThermoFisher cat #FD0694) and using T4 DNA ligase (ThermoFisher cat #EL0014) was cloned into pBAD/HisA expression vector (ThermoFisher cat #V43001) precleaved with NheI (ThermoFisher cat #FD0973) and XhoI and dephosphorylated using FastAP (ThermoFisher cat #EF0651). The GsSir2 protein contains a His_6-Tag at its N terminus. The mutants DSR2 (N133A) and DSR2 (H171A) were constructed using the Q5 Site-directed Mutagenesis kit (NEB, E0554S) using either primers JG216 and JG217, or JG220 and JG221 respectively. The mutant DSR1 (H194A) was constructed using the Q5 Site-directed Mutagenesis kit using primers JG496 and JG497. The mutant SIR2-HerA (SIR2 D165A H212A) was constructed by first using the Q5 Site-directed Mutagenesis kit using primers JG498 and JG499 to introduce the D165A mutation, and then using the resulting plasmid for further Q5 Site-directed Mutagenesis and the introduction of the second H212A mutation using primers JG500 and JG501. The mutant SIR2-HerA (HerA K167A) was constructed using the Q5 Site-directed Mutagenesis kit using primers JG502 and JG503. The mutant SIR2/pAgo (SIR2 N142A) was constructed using the Q5 Site-directed Mutagenesis kit using primers JG463 and JG464.To inactivate the GsAgo protein a bulky His_6-**S**trepII-His_6-tag (HSH-tag, 29 aa.: LEGHHHHHHSSWSHPQFEKGVEGHHHHHH) was fused to its C terminus. For this, a whole operon of the GsSir2/Ago system was amplified by PCR using the oligonucleotides MZ-325 and MZ-326, respectively, from the genomic DNA. The resulting DNA fragment was digested by Eco31I and XhoI and using T4 DNA ligase was cloned into pBAD24-HSH expression vector

precleaved with NcoI (ThermoFisher cat#FD0573) and XhoI and dephosphorylated using FastAP. In this case, the GsSir2 protein does not contain any tag at its N-terminus.

A cloning shuttle vector for large fragments was constructed by Genscript Corp. This vector was constructed by replacing the Pxyl promoter and its downstream open reading frame in plasmid pGO1_thrC_Pxyl_cereus_ThsA [7], with a synthesized Phspank sfGFP cassette taken from pDR111 [24], resulting in the plasmid pSG-thrC_Phspank_sfGFP (Supplementary File S2). The vector contains a p15a origin of replication and ampicillin resistance for plasmid propagation in *E. coli*, and a thrC integration cassette with chloramphenicol resistance for genomic integration into *B. subtilis*.

DSAD1 from SPbeta (NCBI protein accession WP_004399562) and phage tail tube protein from SPR (NCBI protein accession WP_010328117) were amplified from phage genomic DNA using primers JG346 and JG347 (for DSAD1) and JG142 and JG143 (for tail tube), and cloned into the pSG-thrC_Phspank_sfGFP vector, replacing sfGFP. The vector backbone was amplified using primers JG13 and JG14.

The additional DSR2 activator candidates tested in this research were also amplified from phage SPR genomic DNA and cloned into the pSG-thrC_Phspank_sfGFP vector, replacing sfGFP. “Operon 1” was lifted with JG431 and J432. “Operon 2” was lifted with JG433 and JG434. “Operon 3” was lifted with JG435 and JG436. “gene 5” was lifted with JG437 and JG438. “gene 6” was lifted with JG439 and JG440. “gene 7” was lifted with JG441 and JG442.

In a similar fashion, the additional DSR2 inhibition candidates tested in this paper were amplified from phage SPbeta. “gene 1” was lifted with JG134 and JG183. “gene 2” was lifted with JG184 and JG185. “gene 3” was lifted with JG186 and JG187. “gene 4” was lifted with JG188 and JG189.

For expression in *E. coli MG1655*, DSR2 and DSR2(H171A) were amplified and cloned into the plasmid pBbA6c-RFP (Addgene, cat. #35290) using primers JG259 and JG260. The SPR tail tube gene was amplified from phage genomic DNA and cloned into the plasmid pBbS8k-RFP (Addgene, cat. #35276) with primers JG249 and JG250 for inducible expression in *E. coli*.

For the assembly of tagged protein constructs, a pBbS8k with sfGFP fused to a C-terminal TwinStrep tag was first constructed (Supplementary File S3). The pBbS8k vector backbone was amplified using primers JG406 and JG407, and the sfGFP with a C-terminal TwinStrep tag was amplified from an *amyE* shuttle vector pGO6_amyE_hspank_GFP [7] with primers JG366 and JG367 and cloned into the pBbS8k plasmid, replacing RFP. To create the C-terminally-tagged SPR tail tube, SPbeta tail tube and DSAD1 constructs, the genes were amplified from phage genomic DNA using primers JG408 and JG409 (for SPR tail tube), JG421 and JG422 (for SPbeta tail tube) and JG410 and JG411 (for DSAD1) and cloned into the pBbS8k sfGFP with C-terminal TwinStrep mentioned above, replacing sfGFP. For this, the pBbS8k with C-terminal TwinStrep vector backbone was amplified using primers JG407 and JG412.

For the assembly of a DSAD1 gene containing plasmid which is compatible with both pBbS8k and pBbA6c, DSAD1 gene was lifted from phage SPbeta genomic DNA using primers JG429 and

JG430 and Gibson assembled with a backbone amplified from plasmid pAraGFPCDF (Addgene, cat. #47516) with primers JG427 and JG428.

To assemble a constitutively expressed pVip construct to be integrated into the thrC site of *B. subtilis*, first the pVip gene was lifted from the plasmid reported in [13] using primers JG3 and JG4 and Gibson assembled with a backbone amplified from plasmid pJMP4 (provided by J. M. Peters) with primers JG1 and JG2. From the resulting plasmid, pVIP was lifted with the Pveg promoter using primers JG82 and JG83 and Gibson assembled with a backbone amplified from pSG-thrC_Phspank_sfGFP using primers JG81 and OGO603.

All PCR reactions were performed using KAPA HiFi HotStart ReadyMix (Roche cat # KK2601). Cloning was performed using the NEBuilder HiFi DNA Assembly kit (NEB, E2621).

Bacillus transformation

Transformation to *B. subtilis* BEST7003 was performed using MC medium as previously described [25]. MC medium was composed of 80 mM K_2HPO_4, 30 mM KH_2PO_4, 2% glucose, 30 mM trisodium citrate, 22 µg/ml ferric ammonium citrate, 0.1% casein hydrolysate (CAA), 0.2% sodium glutamate. From an overnight starter of bacteria, 10 µl were diluted in 1 ml of MC medium supplemented with 10 µl 1M $MgSO_4$. After 3 hours of incubation (37°C, 200 rpm), 300 µl of the culture was transferred to a new 15 ml tube and ~200 ng of plasmid DNA was added. The tube was incubated for another 3 hours (37°C, 200 rpm), and the entire reaction was plated on Lysogeny Broth (LB) agar plates supplemented with 5 µg/ml chloramphenicol or 100 µg/ml spectinomycin and incubated overnight at 30°C.

Plaque assays

Phages were propagated by picking a single phage plaque into a liquid culture of *B. subtilis* BEST7003 or *E. coli* MG1655 grown at 37°C to OD_{600} 0.3 in MMB medium until culture collapse. The culture was then centrifuged for 10 minutes at 3,200 x *g* and the supernatant was filtered through a 0.2 µm filter to get rid of remaining bacteria and bacterial debris. Lysate titer was determined using the small drop plaque assay method as previously described [26].

Plaque assays were performed as previously described [6,26]. Bacteria containing defense system and control bacteria with no system were grown overnight at 37°C. Then 300 µl of the bacterial culture was mixed with 30 ml melted MMB 0.5% agar, poured on 10 cm square plates, and let to dry for 1 hour at room temperature. For cells that contained inducible constructs, the inducers were added to the agar before plates were poured. 10-fold serial dilutions in MMB were performed for each of the tested phages and 10 µl drops were put on the bacterial layer. After the drops had dried up, the plates were inverted and incubated overnight at room temperature or 37°C. Plaque forming units (PFUs) were determined by counting the derived plaques after overnight incubation and lysate titer was determined by calculating PFUs per ml. When no individual plaques could be identified, a faint lysis zone across the drop area was considered to be 10 plaques. Details of specific conditions used in plaque assays for each defense system are found in Table 2.

Liquid culture growth assays

Non-induced overnight cultures of bacteria containing defense system and bacteria with no system (negative control) were diluted 1:100 in MMB medium supplemented with appropriate antibiotics

and incubated at 37°C while shaking at 200 rpm until early log phase (OD_{600} = 0.3). 180 µl of the culture were then transferred into wells in a 96-well plate containing 20 µl of phage lysate for a final MOI of 10 and 0.1 for phage lambda(vir), an MOI of 4 and 0.04 for phages SPR, phi29 and vB_EcoM-KAW1E185, or 20 µl of MMB for uninfected control. Infections were performed in triplicates from overnight cultures prepared from separate colonies. Plates were incubated at 30°C or 37°C (as indicated) with shaking in a TECAN Infinite200 plate reader and an OD_{600} measurement was taken every 10 min. Details of specific conditions used for each defense system are found in Table 2.

Liquid culture growth toxicity assays

Non-induced *E. coli* MG1655 with DSR2 and tail tube, or DSR2 and RFP (negative control), were grown overnight in MMB supplemented with 1% glucose and the appropriate antibiotics. Cells were diluted 1:100 in 3 ml of fresh MMB and grown at 37°C to an OD_{600} of 0.3 before expression was induced. The inducers were then added to a final concentration of 0.2% arabinose and 1mM IPTG, and MMB was added instead for the uninduced control cells. The cells were transferred into a 96-well plate. Plates were incubated at 37°C with shaking in a TECAN Infinite200 plate reader with an OD_{600} measurement was taken every 10 min.

Infection time course phage titer assay

Non-induced overnight cultures of bacteria containing the DSR2 gene and bacteria with no system (negative control) were diluted 1:100 in 3 ml MMB medium and incubated at 37°C while shaking at 200 rpm until early log phase (OD_{600} = 0.3), and then cultures were infected with phage SPR at an MOI of 4. Cultures were left shaking at 37°C for the duration of the experiment. At each time point, 1 ml of culture was filtered through a 0.2 µm filter (Whatman cat# 10462200) and then used in an infection plaque assay on *B. subtilis* BEST7003 at room temperature. The sample for time 0 was produced my mixing the same amount of phage used for infection in 3 ml MMB medium.

Cell lysate preparation for LC-MS

Overnight cultures of bacteria containing defense systems and bacteria with no system (negative control) were diluted 1:100 in 250 ml MMB and incubated at 37°C with shaking (200 rpm) until reaching OD_{600} of 0.3. For cells that contained inducible SIR2/pAgo constructs, the inducers were added at an OD_{600} of 0.1. A sample of 50 ml of uninfected culture (time 0) was then removed, and phage stock was added to the culture to reach an MOI of 5-10. Flasks were incubated at 30°C or 37°C (as indicated) with shaking (200 rpm) for the duration of the experiment. 50 ml samples were collected at various time points post infection. Immediately upon sample removal the sample tube was placed in ice, and centrifuged at 4°C for 5 minutes to pellet the cells. The supernatant was discarded and the tube was frozen at -80°C. To extract the metabolites, 600 µl of 100 mM phosphate buffer at pH 8, supplemented with 4 mg/ml lysozyme, was added to each pellet. Tubes were then incubated for 30 minutes at RT, and returned to ice. The thawed sample was transferred to a FastPrep Lysing Matrix B 2 ml tube (MP Biomedicals cat # 116911100) and lysed using FastPrep bead beater for 40 seconds at 6 m/s. Tubes were then centrifuged at 4°C for 15 minutes at 15,000 *g*. Supernatant was transferred to Amicon Ultra-0.5 Centrifugal Filter Unit 3 KDa (Merck Millipore cat # UFC500396) and centrifuged for 45 minutes at 4°C at 12,000 *g*. Filtrate was taken and used for LC-MS analysis. Details of specific conditions used for each defense system are found in Table 2.

Quantification of NAD^+ and ADPR by HPLC-MS

Cell lysates were prepared as described above and analyzed by LC-MS/MS. Quantification of metabolites was carried out using an Acquity I-class UPLC system coupled to Xevo TQ-S triple quadrupole mass spectrometer (both Waters, US). The UPLC was performed using an Atlantis Premier BEH C18 AX column with the dimension of 2.1 × 100 mm and particle size of 1.7 µm (Waters). Mobile phase A was 20 mM ammonium formate at pH 3 and acetonitrile was mobile phase B. The flow rate was kept at 300 µl min^{-1} consisting of a 2 min hold at 2% B, followed by linear gradient increase to 100% B during 5 min. The column temperature was set at 25°C and an injection volume of 1 µl. An electrospray ionization interface was used as ionization source. Analysis was performed in positive ionization mode. Metabolites were detected using multiple-reaction monitoring, using argon as the collision gas. Quantification was made using standard curve in 0–1 mM concentration range. NAD+ (Sigma, N0632-1G) and ADPR (Sigma, A0752-25MG) were added to standards and samples as internal standard (0.5 µM). TargetLynx (Waters) was used for data analysis.

Pulldown assays

Non-induced overnight cultures of *E. coli* MG1655 with DSR2 (H171A), DSAD1, DSAD1 with C-terminal TwinStrep tag, SPR tail tube protein with C-terminal TwinStrep tag, or combinations of these proteins were diluted 1:100 in 50 ml of MMB and grown at 37°C to an OD_{600} of 0.3. Expression was then induced by adding 0.2% arabinose and 1mM IPTG, and cells continued to grow to an OD_{600} of 0.9 at 37°C. Cells were centrifuged at 3,200 x *g* for 10 minutes. Supernatant was discarded and pellets were frozen in -80°C.

To pull down the proteins, 1 ml of Strep-Tactin wash buffer (IBA cat # 2-1003-100) supplemented with 4 mg/ml lysozyme was added to each pellet and incubated for 10 minutes at 37°C with shaking until thawed, and then resuspended. Tubes were then transferred to ice, and the resuspended cells transferred to a FastPrep Lysing Matrix B in 2 ml tube (MP Biomedicals cat # 116911100). Samples were lysed using FastPrep bead beater for 40 seconds at 6 m/s. Tubes were centrifuged for 15 minutes at 15,000 x g. Per each pellet, 30 µl of MagStrep "Type 3" XT beads (IBA cat # 2-4090-002) were washed twice in 300 µl wash buffer (IBA cat # 2-1003-100), and the lysed cell supernatant was mixed with the beads and incubated for 30-60 minutes, rotating at 4°C. The beads were then pelleted on a magnet, washed twice with wash buffer, and purified protein was eluted from the beads in 10 µl of BXT elution buffer (IBA cat # 2-1042-025). 30 µl of samples were mixed with 10 µl of 4X Bolt™ LDS Sample Buffer (ThermoFisher cat#B0008) and a final concentration of 1mM of DTT. Samples were incubated at 75°C for 5 minutes, and then loaded to a NuPAGE™ 4 to 12%, Bis-Tris, 1.0 mm, Mini Protein Gel, 12-well (ThermoFisher cat# NP0322PK2) in 20X Bolt™ MES SDS Running Buffer (ThermoFisher cat# B0002) and run at 160V. Gels were shaken with InstantBlue® Coomassie Protein Stain (ISB1L) (ab119211) for 1 hour, followed by another hour in water. All bands shown in Fig. 3B were verified to represent the indicated protein by mass spectrometry.

Phage coinfection and hybrid isolation

50 µl overnight culture of *B. subtilis* containing DSR2 and pVip was mixed with 50 µl of phage SPR and 50 µl of either phi3T or SPbeta, each phage at a titer of 10^7 PFU/ml. Bacteria and phages were left to rest at room temperature for 10 minutes before being mixed with 5ml of premelted MMB 0.3% agar and poured over a plate containing MMB 0.5% agar. Plates were left overnight

at room temperature before being inspected for plaques. Single plaques were picked into 100 µl phage buffer (50 mM Tris-HCl pH 7.4, 100 mM $MgCl_2$, 10 mM NaCl). Hybrid phages were tested for their ability to infect DSR2-containing cells using small drop plaque assay as described above.

Sequencing and assembly of phage hybrids

High titer phage lysates (>10^7 pfu/ml) of the ancestor and isolated phage hybrids were used for DNA extraction. 500 µl of the phage lysate was treated with DNaseI (Merck cat #11284932001) added to a final concentration of 20 µg/ml and incubated at 37°C for 1 hour to remove bacterial DNA. DNA was extracted using the QIAGEN DNeasy blood and tissue kit (cat #69504) starting from the Proteinase-K treatment step to lyse the phages. Libraries were prepared for Illumina sequencing using a modified Nextera protocol as previously described [27]. Reads were de novo assembled using Spades3.14.0 [28] with the 'careful' pipeline option which reduces chances for wrong mismatches and short indels in assemblies of small genomes.

Hybrid phage alignment

Hybrid phage genomes were aligned using SnapGene Version 5.3.2. Each hybrid genome was aligned to phage SPR and areas that did not align were aligned against the other phages in the coinfection experiment in order to verify their origin and gene content.

Statistics & Reproducibility

No statistical method was used to predetermine sample size. Experiments were performed in triplicates unless stated otherwise. Randomization was used for sample injection order in mass spectrometry measurements. No data were excluded from the analyses. The experiments in Fig. 3B and Extended Data Fig.5 were repeated independently twice with similar results.

Data availability

Data that support the findings of this study are available within the Article and its Extended Data. Gene accessions appear in the Methods section of the paper. Plasmid maps of the constructs used for the experiments are attached as Supplementary Files. Source data are provided with this paper.

Acknowledgements

We thank the Sorek laboratory members for comments on the manuscript and fruitful discussion. We also thank Alexander Brandis and Tevie Mehlman from the Weizmann Life Sciences Core Facilities for targeted mass spectrometry analyses, and Alon Savidor from the Israel National Center for Personalized Medicine for protein mass spectrometry. R.S. was supported, in part, by the European Research Council (grants ERC-CoG 681203 and ERC-AdG GA 101018520), Israel Science Foundation (grant ISF 296/21), the Ernest and Bonnie Beutler Research Program of Excellence in Genomic Medicine, the Deutsche Forschungsgemeinschaft (SPP 2330, grant 464312965), the Minerva Foundation with funding from the Federal German Ministry for Education and Research, and the Knell Family Center for Microbiology. V.S. was supported by

the European Social Fund [09.3.3-LMT-K-712-01-0126] under a grant agreement with the Research Council of Lithuania (LMTLT).

Author Contributions Statement

J.G. and R.S led the study and performed all analyses and experiments unless otherwise indicated. A.L performed plaque assay experiments with the SIR2/pAgo defense system. A.B cloned and conducted plaque assays for the pVip defense system. M.Z. and V.S. provided the SIR2/pAgo defense system. S.M. and A.L. cloned and conducted plaque assays for the DSR2, DSR1 and SIR2-HerA defense systems. A.M. and G.A. assisted with sequence analysis and prediction of protein domain functions and point mutations. The manuscript was written by J.G. and R.S. All authors contributed to editing the manuscript, and support the conclusions.

Competing Interests Statement

R.S. is a scientific cofounder and advisor of BiomX and Ecophage. The other authors declare no competing interests.

Tables

Table 1. Phages used in this study

PHAGE	SOURCE	IDENTIFIER	ACCESSION
lambda(vir)	Udi Qimron		NC_001416.1
phi105	*Bacillus* Genetic Stock Center (BGSC)	BGSC (1L11)	HM072038.1
phi29	Deutsche Sammlung von Mikroorganismen und Zellkulturen (DSMZ)	DSM 5546	NC_011048.1
phi3T	*Bacillus* Genetic Stock Center (BGSC)	BGSC (1L1)	KY030782.1
SECphi17	Doron et al., 2018		LT960607.1
SECphi18	Doron et al., 2018		LT960609.1
SPbeta	*Bacillus* Genetic Stock Center (BGSC)	BGSC (1L5)	AF020713.1
SPO1	Deutsche Sammlung von Mikroorganismen und Zellkulturen (DSMZ)	BGSC (1P4)	NC_011421.1
Spp1	Deutsche Sammlung von Mikroorganismen und Zellkulturen (DSMZ)	BGSC (1P7)	NC_004166.2
SPR	*Bacillus* Genetic Stock Center (BGSC)	BGSC (1L56)	
T7	Udi Qimron		NC_001604.1
vB_EcoM-KAW1E185	Deutsche Sammlung von Mikroorganismen und Zellkulturen (DSMZ)	DSM 104099	NC_054922.1

Table 2. SIR2 containing defense systems tested in this study

SYSTEM	HOST STRAIN	NEGATIVE CONTROL	PHAGES USED FOR MS AND LIQUID GROWTH ASSAYS	PHAGES USED FOR INFECTION PLAQUE ASSAYS	TEMP. (°C)	INDUCTION
DSR2	*B. subtilis*	Empty cassette	SPR	phi29, spp1, SPR, SPbeta, phi3T, SPO1, phi105	30	Native promoter
DSR1	*B. subtilis*	Empty cassette	phi29	phi29, spp1, SPR, SPbeta, phi3T, SPO1, phi105	30	Native promoter
SIR2/ PAGO	*E. coli*	Empty pBAD	lambda(vir)	vB_EcoM-KAW1E185, lambda(vir), SECphi18, T7, SECphi17	37	0.2% arabinose
SIR2-HERA	*E. coli*	Empty vector	vB_EcoM-KAW1E185	vB_EcoM-KAW1E185, lambda(vir), SECphi18, T7, SECphi17	37	Native promoter

Fig. Legends

Fig 1. DSR2 is an abortive infection protein that causes NAD^+ depletion in infected cells. (A) Domain organization of DSR2 from *B. subtilis* 29R. Protein accession in NCBI is indicated above the gene. (B) Efficiency of plating (EOP) for three phages infecting the control *B. subtilis* BEST7003 strain (no system) or *B. subtilis* BEST7003 with DSR2 cloned from *B. subtilis* 29R. For phage SPR, EOP is also presented for two mutations in the predicted SIR2 catalytic site. Data represent plaque-forming units (PFU) per milliliter. Bar graphs represent average of three independent replicates, with individual data points overlaid. (C) Liquid culture growth of DSR2-containing *B. subtilis* and control *B. subtilis* (no system), infected by phage SPR at 30 °C. Bacteria were infected at time 0 at an MOI of 4 or 0.04. Three independent replicates are shown for each MOI, and each curve represents an individual replicate. (D-E) Concentrations of NAD^+ and ADPR in cell lysates extracted from SPR-infected cells as measured by targeted LC-MS with synthesized standards. X-axis represents minutes post infection, with zero representing non-infected cells. Cells were infected by phage SPR at a MOI of 5 at 30 °C. Bar graphs represent the average of two biological replicates, with individual data points overlaid. Colors are as in panel B.

Fig 2. Genetic exchange between phages reveal regions responsible for escape from DSR2. (A) Genome comparison of phages SPR, SPbeta and phi3T was performed using clinker [29]. Grey/black bands connect homologous genes, with shades of grey representing the % of amino acid sequence identity. (B) Schematic representation of the phage mating experiment. *B. subtilis* BEST7003 cells expressing both DSR2 and pVip are co-infected with phage SPR and SPbeta (or phi3T). Recombination between co-infecting phage genomes leads to hybrid phages that can overcome both defense systems and generate plaques. Examination of the genomes of multiple hybrids predicts genomic regions necessary to overcome defense. (C) Plaque assays with either one or two co-infecting phages. Cells expressing both DSR2 and pVip are infected either with

phage SPR (left), phage SPbeta (middle) or both phages (right). (D) Hybrid phage genomes. Each horizontal line represents the genome of a hybrid phage that can overcome DSR2. Green areas are from phage SPR, blue from SPbeta and purple from phi3T. Representative non-redundant hybrid sequences are presented out of 32 sequenced hybrids. Red rectangles outline two areas that are predicted to allow the phage to overcome DSR2 defense. Top zoom inset shows genes found in the region acquired from phi3T or SPbeta, gene outlined in red codes for DSAD1. Bottom zoom inset shows genes present in the original SPR genome, outlined gene is the tail tube protein.

Fig 3. Phage proteins that activate and inhibit DSR2. (A) DSAD1 inhibits DSR2 defense. Liquid culture growth of *B. subtilis* BEST7003 cells expressing either DSR2 alone, DSAD1 alone, or DSR2 and DSAD1, or control cells expressing neither gene, infected by phage SPR at 30 °C. Three independent replicates are shown. (B) Pulldown assays of the DSR2-DSAD1 and DSR2-tail tube complexes. DSAD1, the tail tube proteins, and control GFP were C-terminally tagged, and co-expressed with DSR2. DSR2 in this experiment was mutated (H171A) to avoid toxicity. Shown is an SDS-PAGE gel. (C) Transformation efficiencies of a vector containing the SPR tail tube protein or GFP control were measured for cells containing either WT DSR2 or two inactive DSR2 mutants. Y-axis represents the number of colony-forming units per milliliter. Bar graphs represent average of three replicates, with individual data points overlaid. (D) Liquid culture growth of *E. coli* that contains DSR2 and the tail tube gene of phage SPR, each under the control of an inducible promoter, and control *E. coli* that contains inducible GFP and DSR2 genes. Expression of both genes was induced at time 0. Three independent replicates are shown. (E-F) Concentrations of NAD^+ and ADPR in cell lysates extracted from *E. coli* co-expressing DSR2 and SPR tail tube. X-axis represents minutes post expression induction, with zero representing non-induced cells. Control cells in this experiment express RFP and DSR2. Bar graphs represent the average of two biological replicates, with individual data points overlaid. (G) A model for the mechanism of action of DSR2. Phage infection is sensed by the recognition of the phage tail tube protein through direct binding to DSR2. This triggers the enzymatic activity of the SIR2 domain to deplete the cell of NAD^+ thereby causing abortive infection. The phage anti-DSR2 protein DSAD1 inhibits DSR2 by direct binding.

Fig 4. SIR2-containing defense systems deplete NAD^+ in infected cells. (A) Domain organization of three defense systems that contain SIR2 domains. Protein accessions in NCBI are indicated. (B) Efficiency of plating for phages infecting defense-system-containing strains and control strains. SIR2-HerA and SIR2/pAgo were cloned into *E. coli* MG 1655, and DSR1 was cloned into *B. subtilis* BEST7003. Bar graphs are average of three biological replicates, with individual data points overlaid. KAW1E185 is short for vB_EcoM-KAW1E185, a T4-like phage. Asterisk marks statistically significant decrease (Student's t-test, two-sided, p-values = 0.005, 0.036, 0.025, for phages lambda (vir), KAW1E185, phi29, respectively). (C-E) Concentrations of NAD^+ in cell lysates extracted from infected cells as measured by targeted LC-MS with synthesized standards. X-axis represents minutes post infection, with zero representing non-infected cells. "No system" are control cells that contain an empty vector instead of the defense system. Bar graphs represent the average of two biological replicates, with individual data points overlaid. (F-H). Liquid culture growth of bacteria that contain the respective defense system and control bacteria that contain an empty vector (no system). Bacteria were infected at time 0 at low or high MOIs, as indicated. Three independent replicates are shown for each MOI, and each curve shows an individual replicate.

References

1. North, B. J. & Verdin, E. Protein family review Sirtuins : Sir2-related NAD-dependent protein deacetylases. *Genome Biol* **5**, 224 (2004).
2. Imai, S., Armstrong, C. M., Kaeberlein, M. & Guarente, L. Transcriptional silencing and longevity protein Sir2 is an NAD-dependent histone deacetylase. *Nature* **403**, 795–800 (2000).
3. Tanny, J. C., Dowd, G. J., Huang, J., Hilz, H. & Moazed, D. An Enzymatic Activity in the Yeast Sir2 Protein that Is Essential for Gene Silencing. *Cell* **99**, 735–745 (1999).
4. Dang, W. & Pfizer, N. C. The controversial world of sirtuins. *Drug Discov. Today Technol.* **12**, e9–e17 (2014).
5. Makarova, K. S., Wolf, Y. I., Oost, J. Van Der & Koonin, E. V. Prokaryotic homologs of Argonaute proteins are predicted to function as key components of a novel system of defense against mobile genetic elements. *Biol. Direct* **4**, 29 (2009).
6. Doron, S. *et al.* Systematic discovery of antiphage defense systems in the microbial pangenome. *Science* **359**, eaar4120 (2018).
7. Ofir, G. *et al.* Antiviral activity of bacterial TIR domains via signaling molecules that trigger cell death. *Nature* **600**, 116–120 (2021).
8. Gao, L. *et al.* Diverse enzymatic activities mediate antiviral immunity in prokaryotes. *Science* **369**, 1077–1084 (2020).
9. Lopatina, A., Tal, N. & Sorek, R. Abortive Infection : Bacterial Suicide as an Antiviral Immune Strategy. *Annu. Rev. Virol.* **7**, 371–384 (2020).
10. Kohm, K. & Hertel, R. The life cycle of SPβ and related phages. *Arch. Virol.* **166**, 2119–2130 (2021).
11. Noyer-Weidner, M., Jentsch, S., Pawlek, B., Günthert, U. & Trautner, T. A. Restriction and modification in Bacillus subtilis: DNA methylation potential of the related bacteriophages Z, SPR, SP beta, phi 3T, and rho 11. *J. Virol.* **46**, 446–453 (1983).
12. Dragoš, A. *et al.* Pervasive prophage recombination occurs during evolution of spore-forming Bacilli. *ISME J.* **15**, 1344–1358 (2021).
13. Bernheim, A. *et al.* Prokaryotic viperins produce diverse antiviral molecules. *Nature* **589**, 120–124 (2021).
14. Freire, D. M. *et al.* An NAD+ Phosphorylase Toxin Triggers Mycobacterium tuberculosis Cell Death. *Mol. Cell* **73**, 1282-1291.e8 (2019).
15. Morehouse, B. R. *et al.* STING cyclic dinucleotide sensing originated in bacteria. *Nature* **586**, 429–433 (2020).
16. Skjerning, R. B., Senissar, M., Winther, K. S., Gerdes, K. & Brodersen, D. E. The RES domain toxins of RES-Xre toxin-antitoxin modules induce cell stasis by degrading NAD+. *Mol. Microbiol.* **111**, 221–236 (2019).
17. Tang, J. Y., Bullen, N. P., Ahmad, S. & Whitney, J. C. Diverse NADase effector families mediate interbacterial antagonism via the type VI secretion system. *J. Biol. Chem.* **293**, 1504–1514 (2018).
18. Tal, N. *et al.* Cyclic CMP and cyclic UMP mediate bacterial immunity against phages. *Cell* **184**, 5728-5739.e16 (2021).
19. Millman, A. *et al.* Bacterial Retrons Function In Anti-Phage Defense. *Cell* **183**, 1551-1561.e12 (2020).
20. Kaufmann, G. Anticodon nucleases. *Trends Biochem. Sci.* **25**, 70–74 (2000).

21. Depardieu, F. *et al.* A Eukaryotic-like Serine/Threonine Kinase Protects Staphylococci against Phages. *Cell Host Microbe* **20**, 471–481 (2016).
22. Millman, A. *et al.* An expanding arsenal of immune systems that protect bacteria from phages. Preprint at https://www.biorxiv.org/content/10.1101/2022.05.11.491447v1 (2022).
23. Cohen, D. *et al.* Cyclic GMP–AMP signalling protects bacteria against viral infection. *Nature* **574**, 691–695 (2019).
24. Overkamp, W. *et al.* Benchmarking various green fluorescent protein variants in Bacillus subtilis, Streptococcus pneumoniae, and Lactococcus lactis for live cell imaging. *Appl. Environ. Microbiol.* **79**, 6481–6490 (2013).
25. Wilson, G. A. & Bott, K. F. Nutritional Factors Influencing the Development of Competence in the Bacillus subtilis Transformation System. *J. Bacteriol.* **95**, 1439–1449 (1968).
26. Mazzocco A, Waddell TE, Lingohr E, J. R. Enumeration of bacteriophages using the small drop plaque assay system. *Methods Mol. Biol.* **501**, 81–85 (2009).
27. Baym, M. *et al.* Inexpensive multiplexed library preparation for megabase-sized genomes. *PLoS One* **10**, e0128036 (2015).
28. Prjibelski, A., Antipov, D., Meleshko, D., Lapidus, A. & Korobeynikov, A. Using SPAdes De Novo Assembler. *Curr. Protoc. Bioinforma.* **70**, 1–29 (2020).
29. Gilchrist, C. L. M. & Chooi, Y.-H. Clinker & Clustermap.Js: Automatic Generation of Gene Cluster Comparison Figures. *Bioinformatics* **37**, 2473–2475 (2021).
30. Gabler, F. *et al.* Protein Sequence Analysis Using the MPI Bioinformatics Toolkit. *Curr. Protoc. Bioinforma.* **72**, 1–30 (2020).
31. Zaremba, M. *et al.* Sir2-domain associated short prokaryotic Argonautes provide defence against invading mobile genetic elements through NAD+ depletion. Preprint at https://www.biorxiv.org/content/10.1101/2021.12.14.472599v1 (2021).
32. Altschul, S. F. *et al.* Gapped BLAST and PSI-BLAST: A new generation of protein database search programs. *Nucleic Acids Res.* **25**, 3389–3402 (1997).